Volume 44, Number 3, 2018.

Mobility & Vehicle Mechanics

International Journal for Vehicle Mechanics, Engines and Transportation Systems

ISSN 1450 - 5304

UDC 621 + 629(05)=802.0

UNIVERSITY OF KRAGUJEVAC, FACULTY OF ENGINEERING

SERBIAN SOCIETY OF AUTOMOTIVE ENGINEERS

M V M **M**obility **V**ehicle **M**echanics

Editors: Prof. dr ***Jovanka Lukić****; Prof. dr* ***Čedomir Duboka***

MVM *Editorial Board*
University of Kragujevac
Faculty of Engineering
Sestre Janjić 6, 34000 Kragujevac, Serbia
Tel.: +381/34/335990; Fax: + 381/34/333192

For Publisher: Prof. dr Dobrica Milovanović, dean, University of Kragujevac, Faculty of Engineering

Publishing of this Journal is financially supported from:
Ministry of Education, Science and Technological Development, Republic Serbia

Mobility &
Vehicle
Mechanics

Volume 44
Number 3
2018.

Motorna
Vozila i
Motori

Mobility & **V**ehicle **M**echanics

Volume 44
Number 3
2018.

Motorna **V**ozila i **M**otori

MOBILITY & VEHICLE MECHANICS

DOI:10.24874/mvm.2018.44.03.01
UDC:629.33:004.94

COMPARATIVE ANALYSIS OF CAR FOLLOWING MODELS BASED ON DRIVING STRATEGIES USING SIMULATION APPROACH

Vase Jordanoska [1], Igor Gjurkov [2], Darko Danev [3]*

Received in August 2018 Accepted in September 2018

RESEARCH ARTICLE

ABSTRACT: Transportation and traffic affect all the aspects of everyday life. To better understand traffic dynamics traffic models are developed. On microscopic level, car-following models are developed and improved during long period of time. They are used in traffic simulation tools or are the basis for operation in some advanced vehicle systems. Car-following models describe traffic dynamics through movement of individual vehicle-driver units. This paper compares Gipps model and Intelligent Driver Model (IDM) as car-following models based on driving strategies. These models are derived based on assumptions such as keeping safe distance from the leading vehicle, driving at a desired speed and producing accelerations within a comfortable range. The models are implemented and simulated in MATLAB environment and the results are discussed in terms of the ability to reproduce real driving behaviour in car following scenarios.

KEY WORDS: traffic dynamics, traffic simulation, car-following model, driving behaviour

[1]*Vase Jordanoska, M.Sc.,assist., University Ss. Cyril and Methodius, Faculty of Mechanical Engineering - Skopje, ul. Rugjer Boshkovikj 18, 1000 Skopje, Republic of Macedonia., vase.jordanoska@mf.edu.mk (*Corresponding author)*
[2]*Igor Gjurkov, Ph.D.,prof. University Ss. Cyril and Methodius, Faculty of Mechanical Engineering - Skopje, ul. Rugjer Boshkovikj 18, 1000 Skopje, Republic of Macedonia, igor.gjurkov@mf.edu.mk*
[3]*Darko Danev, Ph.D.,prof. University Ss. Cyril and Methodius, Faculty of Mechanical Engineering - Skopje, ul. Rugjer Boshkovikj 18, 1000 Skopje, Republic of Macedonia, darko.danev@mf.edu.mk*

UPOREDNA ANALIZA MODELA PRAĆENJA VOZILA NA OSNOVU STRATEGIJE VOŽNJE PRIMENOM SIMULACIJA

REZIME: Transport i saobraćaj utiču na sve aspekte svakodnevnog života. Da bi se što bolje razumela saobraćajna dinamika, razvijaju se modeli saobraćaja. Na mikroskopskom nivou, razvijeni su i unapređivani modeli praćenja vozila tokom dugog perioda vremena. Oni su korišćeni u alatima za simulacije saobraćaja ili su bili osnova za rad nekih naprednih sistema vozila. Modeli praćenja vozila opisuju dinamiku saobraćaja preko kretanje pojedinačnih elemenata vozilo-vozač. U ovom radu su uporđeni Gipps-ov model i Inteligentnim modelom vozača (eng. Intelligent Driver Model (IDM)) kao modeli praćenja vozila zasnovani na strategijama vožnje. Ovi modeli su izvedeni na osnovu pretpostavki kao što su: održavanje bezbednog odstojanja od vodećeg vozila, vožnja željenom brzinom i ubrzavanje u granicama komfora. Modeli su razvijeni i testirani u MATLAB okruženju. Dobijeni rezultati su analizirani sa stanovišta mogućnosti ponavljanja stvarnog ponašanja vozača u scenarijima praćenja vozila.

KLJUČNE REČI: dinamika saobaraćaja, simulacija saobraćaja, modeli praćenja vozila, ponašanje vozača

COMPARATIVE ANALYSIS OF CAR FOLLOWING MODELS BASED ON DRIVING STRATEGIES USING SIMULATION APPROACH

Vase Jordanoska, Igor Gjurkov, Darko Danev

1. INTRODUCTION

One of the key elements for good functioning and progress of modern societies is to have an efficient transport system. Limited road capacity and hence frequent traffic jams is the problem many of them face. Expanding road infrastructure is expensive and it cannot be done in dense urban areas. The solution should be sought in more effective usage of existing road infrastructure through application of new technologies. It is how the research area of intelligent transportation system emerged.

To better understand traffic situations and states, mathematical models are developed. These models also enable analysis and definition of traffic and transport problems, and they give possibility of predicting future conditions, as well as development of proposals for solutions. There are a lot of available traffic related data such as acceleration of individual drivers and vehicles, macroscopic data obtained from static detectors complemented by data from GPS, wireless LAN and mobile phone applications which can be used for modelling as well [9]. Experimental measurements also serve as a basis for mathematical modelling.

Traffic dynamics which can be mathematically interpreted, describes the interaction between number of vehicles and drivers. The interaction of complex so-called "driver-vehicle" units, leads to new joint traffic effects which do not depend on the details of the single units. Example can be stop-and-go waves but also more complex spatial – time patterns of congested traffic.

2. TYPES OF TRAFFIC FLOW MODELS

The types of traffic flow models can be divided on different basis, by the level of aggregation (the way in which the reality is presented), by the mathematical structure or by the conceptual aspects. When it comes to traffic models classification it is usually thought of the level of aggregation. According to it there are three ways to mathematically model real traffic events: macroscopic, microscopic and mesoscopic [1, 6, 9]. By the mathematical structure traffic flow models can be represented as partial differential equations, coupled ordinary differential equations, coupled iterated maps, cellular automata, discrete state variables - continuous time or static models. Also, classification can be made by conception foundation, identical versus heterogeneous drivers and vehicles, constant versus variable driving behaviour or single-lane versus multi-lane models.

Macroscopic models describe the traffic flow as the flow of fluids. Dynamic variables are locally aggregated quantities, such as the traffic density $\rho(x,t)$, flow $Q(x,t)$, mean velocity $V(x,t)$ or the change in velocity $\sigma V2(x,t)$. Macroscopic models describe collective phenomena such as the evolution of congested regions or the propagation velocity of traffic waves.

Microscopic models include car-following models and cellular automata. These models describe individual "driver-vehicle" units as particles α, which form the traffic flow. Microscopic models describe the reaction of each driver (acceleration, braking or lane change) depending on the surrounding traffic. Dynamic variables are position $x_\alpha(t)$, velocity $v_\alpha(t)$ and acceleration $\dot{v}_\alpha(t)$ of the vehicle.

Mesoscopic models are hybrids of the microscopic and macroscopic approach. In local field models, parameters of the microscopic model may depend on macroscopic quantities such as traffic density or local velocity and velocity changes.

2.1 Microscopic models

Microscopic traffic flow modelling is based on description of the motion of each individual vehicle which is a part of the traffic stream. It implies modelling the actions i.e. accelerations, decelerations, and lane changes of each driver-vehicle unit in relation to the surrounding traffic.

In cellular automata models variables are discrete. The space is divided into fixed cells and the time is updated at fixed intervals. The status of each cell is 0 ("no vehicle") or 1 ("vehicle" or "part of a vehicle"). Cell occupancy is determined at each time step and depends on the occupation in the previous step.

In this paper the focus of interest are the car-following models which describe traffic dynamics from perspective of individual "driver-vehicle" units. Literally, car-following models describe the behaviour of the driver (vehicle) only in case of interaction with other vehicles, while the free flow is described by a separate model. However, a car-following model is considered complete if it can describe all situations, including acceleration and free flow, following other vehicles in stationary and non-stationary situations, approaching slow or stopped vehicles and a red traffic light. The first car-following models were proposed as early as the 1950's by Reuschel (1950) and Pipes (1953). These two models contained one of the basic elements of modern microscopic modelling which is the minimum distance, from bumper to bumper to the leading vehicle, known as "safe distance", which should be proportional to the speed. The elementary car-following models also include optimal velocity model, full velocity difference model and Newell’s car-following model.

By the logic used car-following models can be classified in three categories [2]:

- Gazis-Herman-Rothery models (GHR) which state that the following vehicle’s acceleration is proportional to the speed of the follower, the speed difference between follower and leader and the space headway.
- Safety distance models which are based on the assumption that the follower always keeps a safe distance to the leader vehicle. These are also known as car-following models based on driving strategies. Model examples that fall into this category are Gipps, IDM, MITSIM model.
- Psycho-physical models use thresholds for, e.g., the minimum speed difference between follower and leader perceived by the follower. These are also known action-point models. Representatives in this category are Wiedemann and Fritzsche models.

Car-following model is implemented in every available traffic simulation tool like VISSIM, Paramics, Aimsun, MITSIMLab, SUMO, etc. [1].

3. CAR FOLLOWING MODELS BASED ON DRIVING STRATEGIES

Car-following models based on driving strategies are derived on assumptions from real driving behaviour such as keeping a safe distance to the leader vehicle, driving with the desired velocity or accelerating in real and comfortable range [9]. The relation between the braking distance and the velocity is also considered.

Driver-vehicle unit α is described with state variables vehicle's position $x\alpha(t)$ and velocity $v\alpha(t)$ in function of time t and vehicle's length $l\alpha$ (figure 1). From the positions and lengths of vehicles, the distance between them is obtained.

$$s_\alpha = x_{\alpha-1} - l_{\alpha-1} - x_\alpha = x_l - l_l - x_\alpha \tag{1}$$

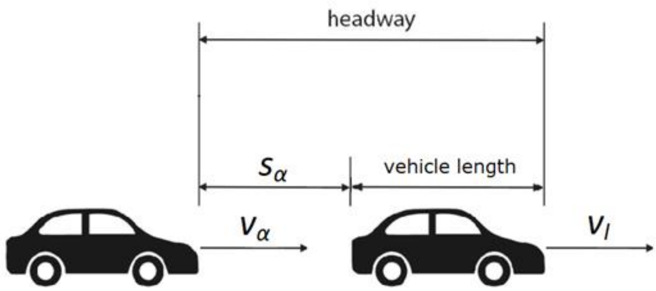

Figure 1. State variables in car-following models

This distance s_α along with vehicles' velocities represents the main input in microscopic models. Of course, depending on the model, additional variables are needed. In time-continuous models driver reaction is given in relation to the acceleration function $a_{mic}(s,v,v_l)$, or when instead of leader velocity v_l, velocity difference ($\Delta v_\alpha = v_\alpha - v_l$) is given, then it is $\tilde{a}_{mic}(s,v,\Delta v)$. In discrete-time models time is not modelled as a continuous variable but is discretized in finite and constant time steps. The driver reaction is given in relation to the velocity function $v_{mic}(s,v,v_l)$.

3.1 Gipps model

Gipps model is named after Peter G. Gipps who developed it in the late 1970's and published it in 1981. The model proposed by Gipps is one of the most extensively used. Studies show that it produces unrealistic acceleration profile because there is no difference between comfortable and maximum braking [3, 4, 9]. Still it is the simplest and complete model without accidents which is accomplished by introducing a safe velocity $v_{safe}(s,v_l)$.

The original formulation of Gipps model states:

$$v(t + \Delta t) = \min[v_{acc}(t + \Delta t), v_{dec}(t + \Delta t)] \tag{2}$$

where

$$v_{acc}(t+\Delta t) = v(t) + 2.5 \cdot a \cdot \Delta t \cdot \left(1 - \frac{v(t)}{v_0}\right) \cdot \sqrt{0.025 + \frac{v(t)}{v_0}} \tag{3}$$

presents the limitation of the acceleration process, and

$$v_{dec}(t+\Delta t) = b \cdot \Delta t + \sqrt{b^2 \cdot \Delta t^2 - 2 \cdot b \cdot (s - s_0) - v(t) \cdot \Delta t - \frac{{v_l}^2}{\hat{b}}} \tag{4}$$

presents the limitation of the braking process. This model is used in traffic simulation package Aimsun and a modified version is used in DRACULA [1]. In 1998 Krauss did a modification of the model which now is used in SUMO traffic simulator [2, 7].

The simplified Gipps model is defined as a discrete-time model with v_{safe} as the main component:

$$v(t+\Delta t) = \min[v + a \cdot \Delta t, v_0, v_{safe}(s, v_l)] \tag{5}$$

where v_0 is the desired velocity.

Braking manoeuvres are performed with constant deceleration b, which means there is no difference between comfortable and maximum deceleration. Braking distance, which the vehicle leader should pass to full stop, is given by $\Delta x_l = v_l^2/2b$.

Constant reaction time Δt exists. So for complete stop of the current vehicle to occur it is not necessary for the vehicle just to pass the braking distance $v^2/2 \cdot b$, but also the additional distance $v \cdot \Delta t$ that is passed during the reaction time: $\Delta x = v \cdot \Delta t + \frac{v^2}{2b}$.

Even in situations where the vehicle leader suddenly slows down and brakes to a full stop, the distance from the vehicle to the vehicle leader should not be less than the minimum defined s_0:

$$s \geq s_0 + v \cdot \Delta t + \frac{v^2}{2b} - \frac{{v_l}^2}{2b} \tag{6}$$

The safe velocity is:

$$v_{safe}(s, v_l) = -b \cdot \Delta t + \sqrt{b^2 \cdot \Delta t^2 + {v_l}^2 + 2 \cdot b \cdot (s - s_0)} \tag{7}$$

3.2 Intelligent Driver Model (IDM)

The intelligent driver model (IDM) is also simple and complete, accident-free model but produces more realistic acceleration profiles. The model is developed by Treiber, Hennecke and Helbing who published it in 2000 [8].

IDM is time-continuous model which has the following characteristics [5, 6]:

The equilibrium distance to vehicle leader cannot be less than the safe distance $s_0+v \cdot T$, where s_0 is minimum distance and T is time gap to the leading vehicle.

It has braking strategy i.e. intelligent control for approaching slower vehicles. Under normal conditions the braking is smooth; the deceleration gradually increases to value b and gradually decreases to 0 before reaching the situation of a steady-state car-following or complete stop. In critical situations deceleration exceeds the comfort value until the danger is avoided.

Transition between driving modes is smooth which means that the time derivative of the acceleration function which is the jerk (m/s^3) is finite at any time. Equivalently, the acceleration function $a_{mic}(s,v,v_l)$ or $\tilde{a}_{mic}(s,v,\Delta v)$ is differentiable by all three variables.

IDM acceleration function has the form $\tilde{a}_{mic}(s, v, \Delta v)$, which is a continuous function of the velocity v, the gap s, and the velocity difference Δv to the leading vehicle:

$$\dot{v} = a\left[1 - \left(\frac{v}{v_0}\right)^2 - \left(\frac{s^*(v,\Delta v)}{s}\right)^2\right] - \mathrm{IDM} \quad (8)$$

and it is consisted of two parts. The first part is comparing the current velocity v with the desired v_0 and the second is comparing the current distance s with the desired s^*.

$$s^*(v,\Delta v) = s_0 + \max\left(0, v\cdot T + \frac{v\cdot\Delta v}{2\cdot\sqrt{a\cdot b}}\right) \quad (9)$$

When there is a situation of an approaching to a stopped vehicle or red traffic light $\Delta v=v$, the equilibrium part $s_0+v\cdot T$ of the dynamical desired distance s^* (Eq. 9) can be neglected and deceleration function gets the form:

$$\dot{v} = -a\left(\frac{s^*}{s}\right)^2 = -\frac{a\cdot v^2\cdot(\Delta v)^2}{4\cdot a\cdot b\cdot s^2} = -\left(\frac{v^2}{2\cdot s}\right)^2\cdot\frac{1}{b} = -\frac{{b_{kin}}^2}{b} \quad (10)$$

which defines kinematic deceleration $b_{kin} = \frac{v^2}{2\cdot s}$. Kinematic deceleration is the minimum deceleration to avoid collision. A critical situation is considered if b_{kin} is being greater than the comfortable deceleration b ($b_{kin}>b$). In regular situation the actual deceleration is less than the kinematic deceleration ($b_{kin}< b$), which means b_{kin} increases over time and approaches the comfortable deceleration.

Intelligent driver model development was mainly been in direction of using it in ACC (Adaptive Cruise Control) systems in vehicles [5, 6, 9].

4. SIMULATION

In order to compare the properties of Gipps and IDM model, both models were implemented in MATLAB script and simulations were performed within the same scenario. The scenario consists of 1km of road in urban conditions that come to intersection from where vehicles can go left or right (T-shaped intersection, figure 2). So, every vehicle which comes to the intersection point needs to stop before it makes the turn maneuver. Five vehicles are included in simulations which last for 120 seconds.

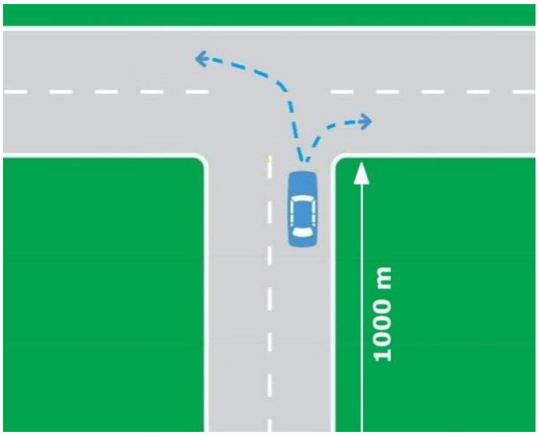

Figure 2. T-shaped intersection

In both car-following models the desired velocity is 54km/h and the minimum distance gap is 2m. The time and the velocity of appearance of a new vehicle in traffic are same in both simulations. The comparative results are given in figure 3. The figure includes results about the gap between vehicles (top graphs), velocities (middle graphs) and accelerations of the vehicles (bottom graphs). Simulation parameters regarding desired velocity, maximum acceleration / deceleration, comfortable deceleration and minimum gap are according to the recommendation of [9].

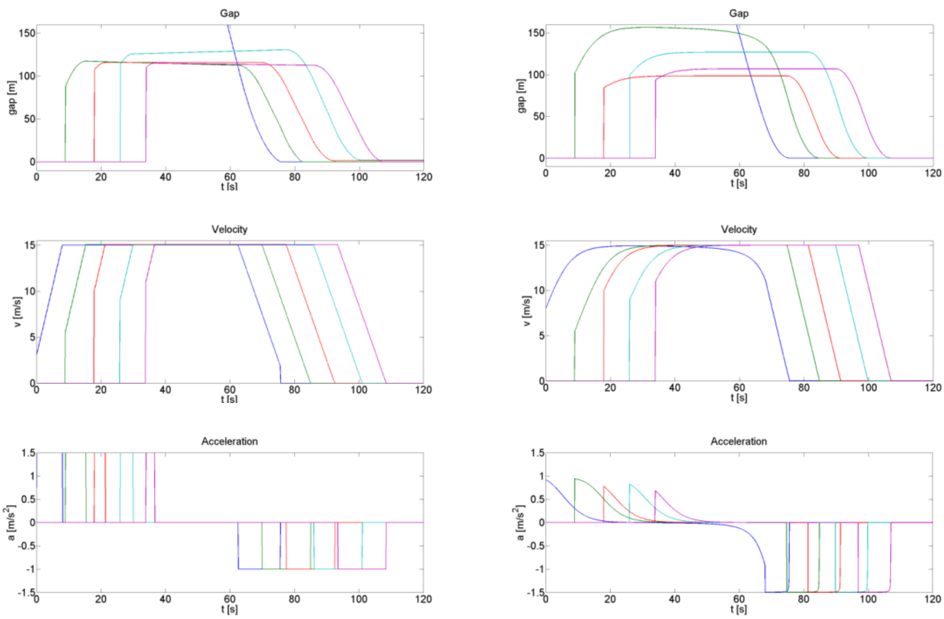

Figure 3. Gipps (left column) and IMD (right column) models' simulation results

In both models, acceleration, car-following and deceleration regimes are clearly visible. In view of simplicity Gipps model produces good results, but the acceleration profile is unrealistic. There are just three acceleration values: a, b and 0. Figure 3 graphs presenting the velocity and the acceleration show resemblance of a robotic driving. Gipps model does not have comfortable and critical deceleration. So if b value is set for critical deceleration, every braking will be done with full braking intensity which is uncomfortable in real driving behaviour. Also, transitions between acceleration / deceleration or no acceleration regimes are hasty and unrealistic.

Intelligent driver model produces more realistic acceleration / deceleration profile but also during the process of acceleration / deceleration the value does not increase gradually. It starts with a maximum (a or b) or near maximum value and then the transition continues smoothly.

As it can be seen from the figure 3 it is a situation with loose traffic. The time interval of appearance of a new vehicle is quite long, up to 8 seconds and the vehicles' gap is large too. If the time of appearance of a new vehicle is reduced the unrealistic acceleration profile of Gipps model is more noticeable (figure 4).

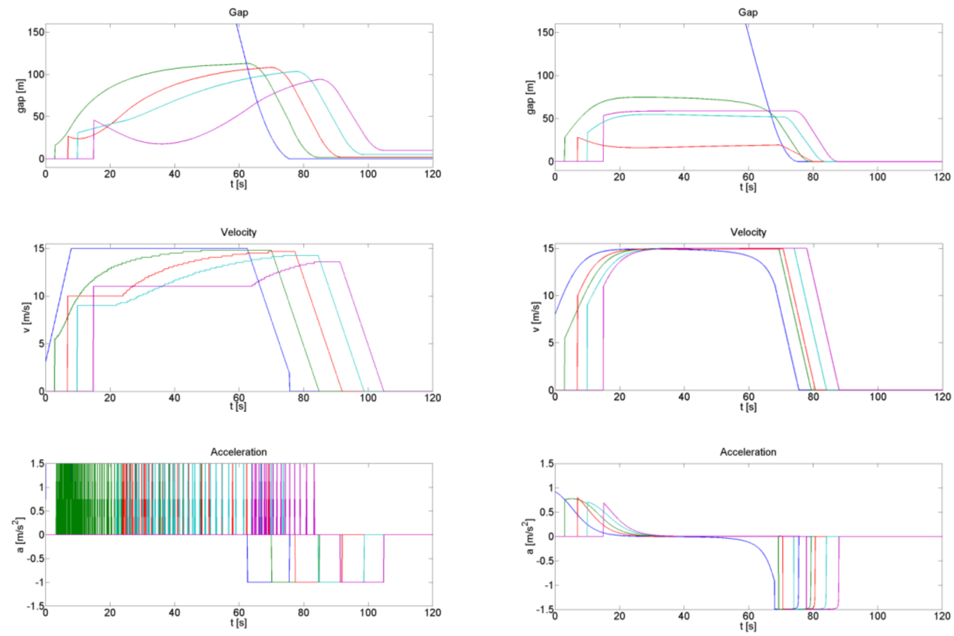

Figure 4. Gipps (left column) and IMD (right column) models' simulation results with a shorter time of appearance

A lot of fluctuations in vehicles' accelerations can be noticed in Gipps model which is not the case in real driving behavior. It is due to the model's formulation which does not include velocity difference between vehicles. The gap between vehicles in Gipps model changes all the time and in IMD it is clearly seen when a vehicle gets into a car-following regime and the desired gap is kept.

5. CONCLUSIONS

Car-following models should reproduce the general behavior of drivers and vehicles in the most realistic way possible. Gipps and IDM are simple and produce accident free results but their disadvantages need to be improved. Because of the unrealistic acceleration Gipps model produces, AIMSUN adopted a modified version which has different strategies for the selection of $\hat{b}$ (the most severe braking that the leading vehicle wishes to undertake), it allows more realistic distances to be kept among vehicles and introduced parameter that can be calibrated [4, 7]. The model used within SUMO is the Gipps model modified by Krauss in 1998, which defines new way of computing the safe velocity. Results of the simulation of Gipps model in MATLAB (given in figure 3 and 4) clearly show that the model gives an unrealistic acceleration profile, which is more apparent when the traffic is dense. When the number of vehicles is higher and the time gap lower, the unrealistic character of the acceleration is more prominent. Regime changes from acceleration mode to car-following mode and vice versa, are harsh. That is not the case in reality, or in the design of autonomous driving. The gap between vehicles in more frequent traffic is constantly changing, and that does not correspond to the objective which is car-following regime in a case of dense traffic.

IDM model gives much better results in terms of acceleration profile, but still improved acceleration function is done in the Improved Intelligent Driver Model (IIDM). The modification is in direction to improve the behavior near the desired speed. Further modifications of the model are done in terms of adapting for ACC systems [5, 6]. Simulation results show that the disadvantage of the intelligent driver model is the initial large acceleration, which would be more realistic if it gradually increases. The same happens in the braking process, with the exception of the first vehicle that moves in free flow regime. In the car-following regime the model produces good results and that can be seen from the gap graph (first row of figure 3 and 4). Comparing the simulation results of both models, it can be concluded that the IDM model produces better results and is more stable than the Gipps model.

In summary, due to its simplicity Gipps model is one of the most used car-following models in traffic modeling and simulations. IDM is a relatively new model, but it is also simple and gives realistic results in terms of the longitudinal parameters of vehicles' dynamics.

REFERENCES

[1] Barceló, J.: "Fundamentals of Traffic Simulation", Springer, 2010, New York.

[2] Brackstone, M., McDonald, M.: "Car-following: a historical review", Transportation Research Part F: Traffic Psychology and Behaviour, Vol. 2, Issue 4, 1999, pp 181-196.

[3] Gipps, Peter G.: "A behavioural car-following model for computer simulation", Transportation Research Part B: Methodological, Vol. 15, Issue 2, 1981, pp 105-111.

[4] Ciuffo, B., Punzo, V., Montanino, M.: "Thirty Years of Gipps' Car-Following Model: Applications, Developments, and New Features", Transportation Research Record: Journal of the Transportation Research Board, Vol. 2315, 2012, pp 89-99.

[5] Kesting, A., Treiber, M., Helbing, D.: "Enhanced intelligent driver model to access the impact of driving strategies on traffic capacity", Philosophical Transactions of the Royal Society of London A: Mathematical, Physical and Engineering Sciences, Vol. 368, 2010, pp 4585-4605.

[6] Kesting, A.: "Microscopic modeling of human and automated driving: Towards traffic-adaptive cruise control", Doctoral Thesis, Technische Universität Dresden, Germany, 2008.

[7] Krajzewicz, D., Christian, R.: "SUMO (Simulation of Urban MObility)-an open-source traffic simulation", Proceedings of the 4th Middle East Symposium on Simulation and Modelling (MESM20002), 2002.

[8] Treiber, M., Hennecke, A., Helbing, D.: "Congested traffic states in empirical observations and microscopic simulations", Physical review E, Vol. 62, 2000, pp 1805-1824.

[9] Treiber, M., Kesting, A.: "Traffic flow dynamics: data, models and simulation", Springer Science & Business Media, 2012.

Intentionally blank

MOBILITY & VEHICLE MECHANICS

DOI:10.24874/mvm.2018.44.03.02
UDC: 658.567.5:581.5

END-OF-LIFE VEHICLE DISPOSAL AND IT'S INFLUENCE TO THE ENVIRONMENT

Saša Mitić [1], Ivan Blagojević [2]*

Received in October 2018 Accepted in October 2018

RESEARCH ARTICLE

ABSTRACT: Motor vehicle industry is nowadays exposed to numerous serious challenges, mostly related to its influence to environment. Motor vehicles during their life cycles affect the environment in several aspects: through consumption of energy and other resources, through production of waste in design process and usage, and through disposal at the end of their life cycle. First two aspects are in consideration for many years and there is noticeable improvement in reducing the effects, but vehicle disposal at the end of life cycle is relatively new area of research. This paper presents main items of international legislative related to end-of-life vehicle recycling process, as well as responsibilities of all participants in this process, from producers to dismantlers and landfills. Also, current legislation in Serbia is presented, with suggestions and ways for future improvement. At the end, concrete data of recyclability and reusability rates for some vehicle models are given, approving the positive effects of applied legislation on vehicle influence to the environment.

KEY WORDS: end-of-life vehicle, recycling, environment, legislative

[1] *Saša Mitić, prof., University of Belgrade, Faculty of Mechanical Engineering, Kraljice Marije 16, 11120, Belgrade, smitic@mas.bg.ac.rs (*Corresponding author)*

[2] *Ivan Blagojević, prof., University of Belgrade, Faculty of Mechanical Engineering, Kraljice Marije 16, 11120, Belgrade, iblagojevic@mas.bg.ac.rs*

ODLAGANJE VOZILA NA KRAJU ŽIVOTNOG VEKA I NJEGOV UTICAJ NA ŽIVOTNU SREDINU

REZIME: Industrija motornih vozila je danas izložena brojnim ozbiljnim izazovima, uglavnom vezanim za njen uticaj na životnu sredinu. Motorna vozila tokom svog životnog ciklusa utiču na životnu sredinu u nekoliko aspekata: kroz potrošnju energije i drugih resursa, kroz proizvodnju otpada u procesu dizajna i upotrebe, i odlaganjem na kraju njihovog životnog ciklusa. Prva dva aspekta se razmatranju već dugi niz godina i vidljivo je poboljšanje u smanjenju efekata, ali odlaganje vozila na kraju životnog ciklusa je relativno nova oblast istraživanja. Ovaj rad predstavlja glavne stavke međunarodnog zakonodavstva vezane za proces recikliranja vozila, kao i odgovornosti svih učesnika u ovom procesu, od proizvođača do demontaže i deponije. Takođe, predstavljeno je sadašnje zakonodavstvo u Srbiji, sa sugestijama i načinima za buduće poboljšanje. Na kraju, dati su konkretni podaci o mogućnosti reciklaže i ponovne upotrebe kod nekih modela vozila, čime je potvrđen pozitivan efekat primenjenog zakonodavstva a tiče se uticaja vozila na životnu sredinu.

KLJUČNE REČI: kraj životnog ciklusa vozila, reciklaža, životna sredina, zakonodavstvo

END-OF-LIFE VEHICLE DISPOSAL AND IT'S INFLUENCE TO THE ENVIRONMENT

Saša Mitić, Ivan Blagojević

1. INTRODUCTION

Vehicle production is continuously growing. Since the end of World War 2, when the global world development and restructuring of the world industries led to growing of the automotive industry, we have constant increase of vehicle production in the world. Following the exact data of produced vehicles in the past, the situation is that from year 1950, when the world production amounts 10 million units, we came up to 58 million units in year 2000 [1]. In next 15 years the increase was more than 50%, so we had more than 90 million vehicles produced in 2015. Report for year 2016 shows 95 million produced vehicles, which indicates further growing of world vehicle production (Figure 1).

End of year 2008 and beginning of 2009 was the only period since 1950 when the drop of vehicle production was recorded, and it was caused by global financial crisis that shaken all industrial and commercial branches. But very quickly, yet in year 2010, increase of vehicle production recovered all reductions from previous year, so again we have constant and stable tendency of vehicle production growing.

Also, all relevant forecasts indicate that this tendency should be kept on in near future.

Regarding the information about vehicles that were sold per year, it was noticeable that their number consistently follows the number of produced vehicles in each year, with slight reduction comparing to them. The only exception was year 2009, when the number of vehicles that were sold surpassed the number of produced vehicles. The reason for that situation was planned reduction of vehicle production and obvious selling of certain number of vehicles from the stocks.

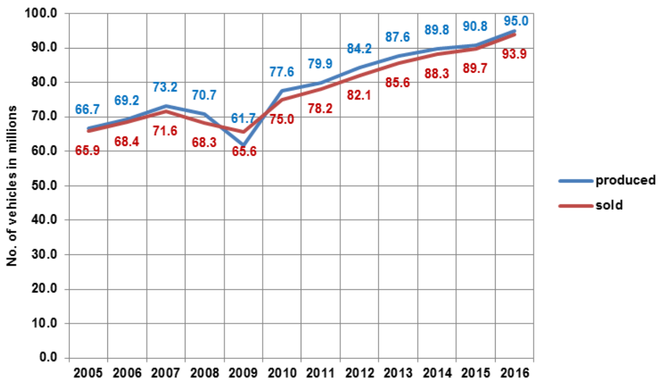

Figure 1. Worlwide vehicle production and selling, period 2005-2016

For further analysis, it is very important to analyze the information about current number of vehicles in use and its structure. This number also increase from year to year, and approximately have the same tendency as the vehicle production. The tendency remains the same for passenger and commercial vehicles (Figure 2).

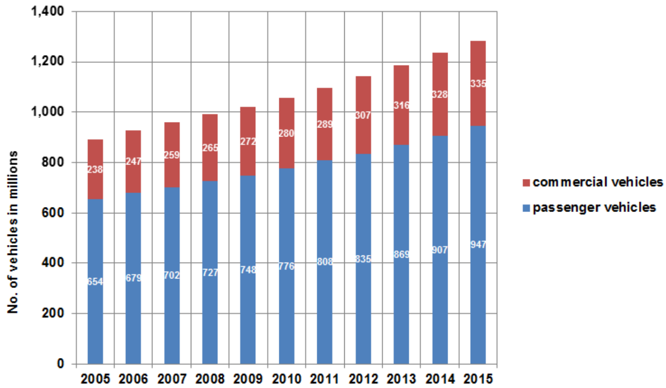

Figure 2. Worldwide vehicle production and selling, period 2005-2015

All previously mentioned indicators unambiguously indicate the importance of research in this field and creation of global strategy for managing the end-of-life vehicles (ELV). According to available data, and if we derive information for year 2015, we come up to the following figures:

- The number of vehicles sold in year 2015 was approximately 90 million units;
- Increase of number of vehicle in use comparing to year 2014 was approximately 47 million units.

The difference between these figures indicates the number of vehicle units in year 2015 that came up to the end of their life cycle, and that number is 43 million units! Negligence of these indicators and not-setting up of appropriate measures could lead us to the situation for our planet to become one big landfill. On the other hand, real situation indicates that the real number of ELVs is probably lower than officially presented. That fact is related to massive export of used vehicles from EU member countries to the rest of Europe (mainly east Europe, Russia, etc.) and some North African countries. Obviously, the profit achieved with vehicle export is much higher, so the problem of ELV treatment EU member countries solve through export. But, the problem of ELV treatment has not been solved, it just has been postponed and transferred to other countries to deal with it [13].

2. INTERNATIONAL LEGISLATIVE

Considerable national policies and voluntary agreements by major automobile manufacturers have been developed concerning the environmental impact of vehicles over their lifetimes. At the end of 1999, ten EU member countries (Austria, Belgium, France, Germany, Italy, the Netherlands, Portugal, Spain, Sweden, and the United Kingdom) had specific regulations and/or industrial voluntary agreements addressing to ELV. These countries represent almost 96% of ELV estimated to be in the European Union [6].

The Directive of European Parliament and of the Council 2000/53/EC of September 18th, 2000 [3] organized former national policies and voluntary agreements. It was aimed to harmonize these existing rules and to push the EU governments and automobile industry to comply fully with the Directive and to translate its key requirements into national laws. The ultimate goal of Directive 2000/53/EC is to put only 5% of ELV residues into landfills. It states:

1. Member States shall take the necessary measures to encourage the reuse of components which are suitable for reuse, the recovery of components which cannot be reused and the giving of preference to recycling when environmentally viable, without prejudice to requirements regarding the safety of vehicles and environmental requirements such as air emissions and noise control;
2. Member States shall take the necessary measures to ensure that the following targets are attained by economic operators:

a) No later than January 1st, 2006, for all ELVs, the reuse and recovery shall be increased to a minimum of 85% by an average weight per vehicle and year. Within the same time limit the reuse and recycling shall be increased to a minimum of 80% by an average weight per vehicle and year; for vehicles produced before January 1st, 1980, Member States may lay down lower targets, but not lower than 75% for reuse and recovery and not lower than 70% for reuse and recycling. Member States making use of this subparagraph shall inform the Commission and the other Member States of the reasons therefore;

b) No later than January 1st, 2015, for all ELVs, the reuse and recovery shall be increased to a minimum of 95% by an average weight per vehicle and year. Within the same time limit, the reuse and recycling shall be increased to a minimum of 85% by an average weight per vehicle and year.

Waste prevention, reuse, recycling, and recovery of the ELV constituents so as to reduce automotive shredding residues (ASR) waste disposal are the objectives of the EC Directive 2000/53/EC. Figure 3 is a schematic representation of the participants in the ELV chain, according to the EU Directive. The main actor is the producer, a vehicle manufacturer or professional importer of a vehicle into a EU member state. The producer links the upstream (supplier) and downstream in the ELV chain (collector, dismantler, and shredder). On the other hand, collaboration between collector, dismantler, and shredder are necessary to successfully meet the directive goals.

The vehicle produced has to at least meet the following goals: low energy consumption, easy dismantling, suitable recycling, and less toxic metals (as shown in Figure 3). To fulfill these goals, the producer has to know the technical and economical facilities, recyclability rate, and efficiencies of the downstream ELV chain. On the other hand, the producer will provide the dismantling information for each new type of vehicle put on the market. The design of vehicles appropriate for dismantling, recycling, and reuse, and free of some hazardous substances (Pb, Hg, Cd, and Cr) will significantly improve the cooperation of the supplier-producer chain [5].

The Directive 2000/53/EC require that the ELV collector and dismantler should be certified (licensed), and as a result, the number of licensed dismantlers in the EU member countries has increased significantly, exceeding 1,000 licensed enterprises per country in the top five producers of vehicles in the EU. The dismantler's role is the removal for sale of reusable parts such as engines, transmissions, gearboxes, and body parts. According to the Directive 2000/53/EC, removing pollutants from the vehicle becomes an important task of the dismantler business. This involves the draining of liquids and removing of environmentally harmful constituents such as the battery. Furthermore, dismantlers are certified to destroy the waste resulting from removing the pollutants (i.e., depollution). These tasks by the dismantler will facilitate the subsequent hulk shredding and will reduce the ASR generated by the shredder operators.

Shredding steps include dismantling small parts for recycling, hulk shredding, and ferrous and non-ferrous metal separation. The separated materials will likely go to automakers for use in the production of the same components from which they are issued. Energy can be recovered from combustible parts of ELV by using them instead of fossil fuels in industrial operations, such as cement plants. The remaining part of the vehicles, ELV waste, will go to a landfill under strict waste control. This will be material for which there is no justification for recovery [8].

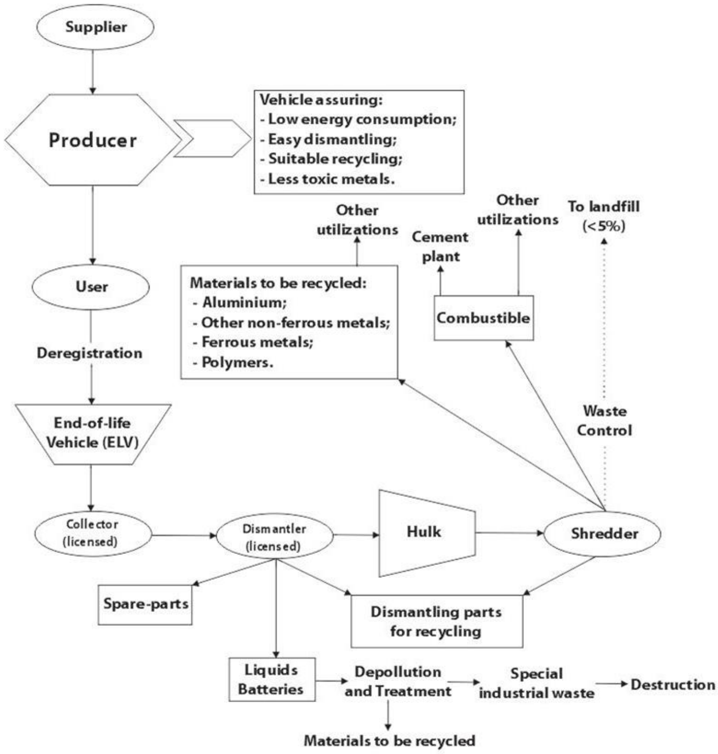

Figure 3. Main steps in ELV recycling process, according to EC Directive 2005/64/EC

EC Directive 2000/53/EC was used as a base for adoption of another Directive, 2005/64/EC [4], which is related to the type-approval of motor vehicles with regard to their reusability, recyclability and recoverability. This Directive strictly prescribe responsibilities of vehicle manufacturers, as well as responsibilities of National Competent Authorities to ensure the fulfillment the Directive's requirements.

Some of the requests related to vehicle manufacturers:

- The manufacturer shall make available to the Type Approval Authority the detailed technical information necessary for the purposes of the calculations and checks, relating to the nature of the materials used in the construction of the vehicle and its component parts
- The manufacturer and the Type Approval Authority jointly identify the reference vehicle in accordance with the criteria prescribed by this Directive
- For the purposes of checks of the materials and masses of component parts, the manufacturer shall make available vehicles and component parts as deemed necessary by the Type Approval Authority

- The manufacturer must be in a position to demonstrate that any version within the vehicle type complies with the requirements of this Directive;
- The manufacturer shall recommend a strategy to ensure dismantling, reuse of component parts, recycling and recovery of materials. The strategy shall take into account the proven technologies available or in development at the time of the application for a Vehicle Type Approval;
- The manufacturer declares measures aiming at the reduction of the quantity and the harmfulness for the environment of end-of life vehicles, their materials and substances.

The competent body shall ensure that the manufacturer has taken the necessary measures to:

- Collect appropriate data through the full chain of supply, in particular the nature and the mass of all materials used in the construction of the vehicles, in order to perform the calculations required under this Directive;
- Keep at its disposal all the other appropriate vehicle data required by the calculation process such as the volume of the fluids, etc.;
- Check adequately the information received from suppliers
- Manage the breakdown of the materials;
- Be able to perform the calculation of the recyclability and recoverability rates in accordance with the standard ISO 22628: 2002 [7];
- Verify that component part prescribed as not to be reused in the construction of new vehicles is reused;
- Mark the component parts made of polymers and elastomers in accordance with Commission Decision 2003/138/EC of February 27th, 2003 establishing component and material coding standards for vehicles pursuant to Directive 2000/53/EC of the European Parliament and of the Council on ELV.

Also, EC Directive 2005/64/EC prescribe the component parts of vehicles belonging to category M1 and those belonging to category N1 which must not be reused in the construction of new vehicles:

- All airbags, including cushions, pyrotechnic actuators, electronic control units and sensors;
- Automatic or non-automatic seat belt assemblies, including webbing, buckles, retractors, pyrotechnic actuators;
- Seats (only in cases where safety belt anchorages and/or airbags are incorporated in the seat);
- Steering lock assemblies acting on the steering column;
- Immobilizers, including transponders and electronic control units;
- Emission after-treatment systems (e.g. catalytic converters, particulate filters);
- Exhaust silencers.

When the vehicle fulfills all requirements regarding the EC Directive 2005/64/EC, which has to be verified with appropriate Test Report, competent authority issue an Approval Certificate. Generally, it means that any new produced vehicle (vehicle of new type) could not be placed into market without valid Approval Certificate.

EC Directive 2005/64 has entered into force in November 2005, starting with application from December 2006, depending of the level of requirement fulfillment. These cases are covered with Transitional provisions.

The same thing is related to requests of UN Regulation 133 [12], which deals with the approval of motor vehicles with regard to their reusability, recyclability and recoverability, within member parties of 1958 Agreement at the World Forum for Harmonization of Vehicle Regulations (WP 29). Since the number of member parties of 1958 Agreement is much higher than EU member countries, the process of harmonization took much more time, so UN Regulation 133 entered into force from June 2014. Comparing with EC Directive 2005/64/EC, it was noticeable that all requirements were almost the same, and it was on the line with EU legislative and UN Regulations harmonization process.

3. NATIONAL LEGISLATIVE

increasing rate. The best indicator is that in last 3 years this branch of industry engage more than 10,000 people. Nowadays there are about 2,200 companies dealing with waste collecting and recycling. Comparing with year 2009, when only 200 companies in this field existed, the improvement is enormous.

Along with engineers and environment experts, recycling industry engages waste collectors all around the country as well. Very often they came from marginalized social groups, so they are covered with social security and included in legal flows.

The way of ELV management in Serbia has not been systematically covered, although nowadays exist approximately 2.3 million registered vehicles, average of 16.5 years. With no integrated and system approach to vehicle recycling, Serbia suffers great loss of resources (materials, energy, employment), and on the other side there are a lot of negative ecological consequences. Serbian trip for joining to EU and status of candidate imposed much more serious approach to this matter than it was in the past.

Relevant national legislative related to ELV management is as follows:

1. Waste Management Law [14];
2. Waste Management Strategy for Period 2010-2019 [15]
3. Methods and Procedures of End-of-Life-Vehicles (ELV) Management Regulation [10].

All 3 main documents were enetered into force in 2010, and generally they were designed for thoroughly covering the whole field of ELV management. Some of main activities scheduled with these documents are [2]:

- Responsibilities of manufacturers, local authorities and all other participants involved into ELV chain
- Procedures to be taken for ELV, from the owner to the landfill
- Keeping the evidence about all steps in ELV management
- Issuing the appropriate documents needed for completing the ELV management procedure
- Short-term and long-term predictions of development process for ELV management
- Predictions about annual amount of waste by categories
- Managing the statistic data regarding the recycling process annually
- To form database of registered and approved vehicle recycling facilities
- Implementing of EC Directives into national legislative documents
- Keeping all financial flows through ELV management under control.

The implementation of legislative is another part of the story, unfortunatelly not very successful at the moment. One of the reasons is previously mentioned fact that this is younges industrial branches in Serbia, faced with numerous problems. The other reason is very slow and difficult process of “mind changing” and acceptance of changes in long-term praxis.

Some of the problems noticed through implementation of new legislative are [9], [11]:

- The treatment of ELV is not in accordance with requirements related to environmental protection
- ELV management system still does not exist as organized activity
- It is still noticeable the presence of dumped vehicle landfills with possibility for people to come and dismantle needed used parts for certain financial compensation
- Domestic manufacturers still do not provide complete information about materials used for vehicle production, coding of components and general information regarding recycling requirements
- There is no designed policy of population education regarding the vehicle recycling
- Penalty policy is still too "soft", and without stronger implementation of legal part of legislative and higher penalties there is no further strong implementation of ELV management efficiently.

4. RECYCLABILITY AND RECOVERABILITY RATES

The method for calculating recyclability and recoverability rates is specified by Standard ISO 22628:2002. It is based on four main stages inspired by the treatment of ELVs. Recyclability and recoverability rates depend on the design and material properties of new vehicles, and on the consideration of proven technologies – those technologies which have been successfully tested, at least on a laboratory scale, in this context.

The calculation method of this Standard cannot reflect the process that will be applied to the road vehicle at the end of its life.

This Standard specifies a method for calculating the recyclability rate and the recoverability rate of a new road vehicle, each expressed as a percentage by mass (mass fraction in percent) of the road vehicle, which can potentially be

- Recycled, reused or both (recyclability rate), or
- Recovered, reused or both (recoverability rate).

The calculation is performed by the vehicle manufacturer when a new vehicle is put on the market.

The calculation of the recyclability and recoverability rates is carried out through the following four steps on a new vehicle, for which component parts, materials or both can be taken into account at each step:

- Pretreatment
- Dismantling
- Metals separation
- Non-metallic residue treatment.

Recyclability rate, Rcyc, of the vehicle, is calculated as a percentage by mass (mass fraction in percent), using the following formula:

$$R_{cyc} = \frac{m_P + m_D + m_M + m_{Tr}}{m_V} \cdot 100 \tag{1}$$

Recoverability rate, R_{cov}, of the vehicle, is calculated as a percentage by mass (mass fraction in percent), using the following formula:

$$R_{cov} = \frac{m_P + m_D + m_M + m_{Tr} + m_{Te}}{m_V} \cdot 100 \qquad (2)$$

where:

m_p –mass of materials taken into account at the pre-treatment step (all fluids, batteries, oil filters, liquefied petroleum gas (LPG) tanks, compressed natural gas (CNG) tanks, tyres, catalytic converters);

m_D –mass of materials taken into account at the dismantling;

m_M –mass of metals taken into account at the metal separation step;

m_{Tr} –mass of materials taken into account at the non-metallic residue treatment step and which can be considered as recyclable;

m_{Te} –mass of materials taken into account at the non-metallic residue treatment step and which can be considered for energy recovery;

m_V –vehicle mass.

For the calculation purposes, a partial mass parameters are determined respectively, at each of these four steps. At the end, the data for the calculation shall be reported using the formalized table review, either on paper or in electronic form. This formalized review has to be presented to the National Type Approval Authority. Also, it presents a part of Information Document that follows Approval Certificate according to EC Directive 2005/64/EC and/or UN Regulation 133. Figure 4 shows completed formalized table for one of the passenger vehicle models, with clear view to all parameters related to material breakdown and mass rates in recycling process.

BRAND NAME	Vehicle Mass m_v (kg)
FORD	1587.6
Model	
C520 FoE , 2017, C520 FoE 15 GTDI B6 RRR V02	

Material-breakdown	Metals (kg)	Polymers (kg)	Elastom. (kg)	Glass (kg)	Fluids (kg)	M.O.N. Mtls (kg)[1]	Others*[2]
	1109.9	271.5	69.9	57.2	70.5	4.8	3.7

[1]: Modified organic natural materials (e.g. leather, wood, cardboard, cotton fleece)
[2]: Other materials (e.g. Electronics and electrics) shall only include components for which the detailed material breakdown cannot easily be established

Pre-Treatment (m_p)			Mass (kg)
	Fluids	m_{P1}	64.3
	Battery	m_{P2}	18.5
	Oil filters	m_{P3}	0.2
	L.P.G. tanks	m_{P4}	0.0
	C.N.G. tanks	m_{P5}	0.0
	Tyres	m_{P6}	46.2
	Catalytic converters	m_{P7}	6.2
		m_P total: (mP1 to mP7)	135.4

Dismantling (m_D)					
Name	Mass (kg)	Name	Mass (kg)	Mass (part 11 to x) (kg)	
				m_D x*	0.0
				* please add a separate list for part 11 to x	
D1 total (Σ1-5):	*0.0*	*D2 total (Σ6-10):*	*0.0*	m_D total: (mD1+mD2+mDx)	0.0

Metal Separation (m_M)			Mass (kg)
	Metal content of the Vehicle	m_M	1109.9
	Metal already div in P and D	m_d	24.4
		m_M: (mM-md)	1085.6

Non Metallic Residue Treatment (m_{Tr} and m_{Te})	m_{Tr} = recyclable materials		Mass (kg)
	Technology no 1	*VW Sicon*	65.0
	Technology no 2		56.7
	Technology no 3		6.7
	*4 to x **		
	* please add a separate list for technologies 4 to x	m_{Tr} total: (S 1-x)	128.4
	m_{Te} = energy recoverable materials		Mass (kg)
	Remaining quantity of organic materials (incl. polymers,elastomers and modified organic natural materials)	m_{Te}:	158.8

Recyclability Rate	$R_{cyc} = \frac{m_P+m_D+m_M+m_{Tr} x\ 100}{m_V} =$	85.0%	1349.4 kg
Recoverability Rate	$R_{cov} = \frac{m_P+m_D+m_M+m_{Tr}+ m_{Te} x\ 100}{m_V} =$	95.0%	1508.2 kg

Reference	Issue Date	Title
C520	25-Apr-2016	Recyclability Calculation ISO 22628
FORD	Revision Date: 06-Feb-2017	Attachment Number: HL-GV41-000057-001

Figure 4. Formalized table review for passenger vehicle (Ford Kuga)

5. CONCLUSIONS

ELV Management became very important part of environmental protection. More and more vehicles are in use and consequently large number of vehicles finishes its life cycle every day, becoming subject of ELV recycling process. Therefore, strong and distinct legislative is needed in order to protect environment. Current international legislative, provide reliable and clear way for ELV managing in the future, but only if it is going to be applied strictly.

Regarding Serbian national legislative, year 2010 was turning point, because 3 main acts were entered into force. Unfortunately, application of legislative is not thorough, hence the effects of possible positive impact are missing. On the other hand some important parts of legislative, especially in "Methods and Procedures of End-of-Life-Vehicles (ELV) Management Regulation" were not written distinctly, so we have different interpretations, and in some cases we have inability to implement them for ELVs because of bad formulations. Therefore, national legislative need to be revised, and much more adopted to international, especially to EC Directive 2005/64/EC and UN Regulation 133.

Having all previously mentioned, main conclusion is imposing by itself: without strong and strict legislative application, it is impossible to keep ELV recycle process under control. Without that control, having in mind enormous number of very old vehicles on the market, Serbia could become big landfill for ELVs, with no possibility to recover for many decades. If we want to avoid that scenario, we need to change our way of thinking, to educate young generations indicating the importance of environment protection and to act "green"

ACKNOWLEDGMENTS

This paper presents some of the results obtained through the project supported by Serbian Ministry of Education, Science and Technological Development (Project No. TR 35045 - "Scientific-Technological Support to Enhancing the Safety of Special Road and Rail Vehicles").

REFERENCES

[1] Statistics of Road Traffic Accidents in Europe and North America, Volume 53, United Nations Economic Commission for Europe, Geneva, 2015.

[2] Ćurčić, S., Paunović, L.: "Recycling of the End-of-Life Motor Vehicles - Situation in Serbia (in Serbian)", Fakultet tehničkih nauka u Čačku, Informacione tehnologije, obrazovanje i preduzetništvo ITOP17, 2017.

[3] Directive 2000/53/EC of the European Parliament and of the Council of 18 September 2000 on end-of life vehicles, Consolidated Version, European Parliament and the Council, Brussels, 2016.

[4] Directive 2005/64/EC of the European Parliament and of the Council of 26 October 2005 on the type-approval of motor vehicles with regard to their reusability, recyclability and recoverability and amending Council Directive 70/156/EEC, Consolidated Version, 02005L0064-20090203, European Parliament and the Council, Brussels, 2009.

[5] Ex-post Evaluation of Certain Waste Stream Directives – Final Report, European Commission – DG Environment, 2014.

[6] Frad, A., Revnic, I.: "ProdTect Automotive – Meeting the Requirements of ELV", International Conference on Engineering Design ICED '07, Paper ID: 245, 2007, Paris, pp 28-31.

[7] ISO 22628:2002 – Road vehicles – Recyclability and recoverability – Calculation method, International Organization for Standardization, Geneva, 2002.

[8] Kanari, N., Pineau, J.-L., Shallari, S.: "End-of-Life Vehicle Recycling in the European Union", The Journal of The Minerals, Metals & Materials Society (TMS), Vol. 55, No. 8, 2003, pp 15-19.

[9] Kozić, A., Sudarević, D.: "Approach to Vehicle Recycling (in Serbian)", 32. Nacionalna konferencija o kvalitetu – Festival kvaliteta, Kragujevac, 2005.

[10] Methods and Procedures of End-of-Life-Vehicles (ELV) Management Regulation (in Serbian), Official Journal 98/2010, Belgrade, 2010.

[11] Pešić, R., Babić, S., Milosavljević, B.: "Recycling in Automobile Industry (in Serbian)", 36. Nacionalna konferencija o kvalitetu – Festival kvaliteta, Kragujevac, 2009.

[12] Regulation No. 133 - Uniform provisions concerning the approval of motor vehicles with regard to their reusability, recyclability and recoverability, The United Nations Economic Commission for Europe (UNECE), Geneva, 2014.

[13] Schneider, J., Karigl, B., Neubauer, C., Tesar, M., Oliva, J., Read, B.: End-of-Life Vehicles: Legal aspects, National Practices and Recommendations for Future Successful Approach, Directorate General for Internal Policies, European Parliament's Committee on Environment, Public Health and Food Safety, 2010.

[14] Waste Management Law (in Serbian), Official Journal 36/2009, 88/2010, Belgrade, 2010.

[15] Waste Management Strategy for Period 2010-2019 (in Serbian), Official Journal 29/2010, Belgrade, 2010.

Intentionally blank

MOBILITY & VEHICLE MECHANICS

DOI: 10.24874/mvm.2018.44.03.03
UDC: 004.94:656.084

A COMPUTATIONAL MODEL FOR THE RECONSTRUCTION OF VEHICLE COLLISIONS

Clio Vossou [1], Dimitrios Koulocheris [2]*

Received in September 2018 Accepted in October 2018

RESEARCH ARTICLE

ABSTRACT: The reconstruction of a vehicle collision consists of the processes of investigation, analysis and conclusions about the causes and the events during the traffic accident. In this perspective, a vehicle collision is considered in three distinct phases, the pre-collision, the collision and the post-collision phase. For the analysis of the collision phase two main approaches exist in the literature, the energy based and the momentum based one. The latter has been described in details by Brach et al. and can find a solution to a given set of parameters to reconstruct a collision. These parameters can be known or assumed using monitoring systems of the vehicle or physical evidence. In the present paper a computational model implementing the Planar Impact Mechanics (PIM) collision model has been set up in Matlab ® and its coupling with the least squares method has been investigated. As test cases, the RICSAC database, which consists of twelve staged collisions, has been used. Special attention has been given in the number of parameters which have been considered known (or assumed). The results indicate the importance of each parameter.

KEY WORDS: traffic accident reconstruction, Planar Impact Mechanics, RICSAC, least squares method, computational model

[1]*Clio Vossou, Researche., National Technical University of Athens, School of Mechanical Engineering, Greece, Zografou Campus, Iroon Polytexneiou 9, 157 80, klvossou@mail.ntua.gr (*Corresponding author)*
[2]*Dimitrios Koulocheris assist. prof., National Technical University of Athens, School of Mechanical Engineering, Greece, Zografou Campus, Iroon Polytexneiou 9, 157 80, dbkoulva@mail.ntua.gr*

PRORAČUNSKI MODEL REKONSTRUKCIJE SUDARA VOZILA

REZIME: Rekonstrukcija sudara vozila se sastoji od procesa: istraživanja, analize i zaključaka o uzrocima i događajima tokom saobraćajne nezgode. Na ovaj način, sudar vozila se razmatra u tri različite faze, pre sudara, tokom sudara i posle sudara. Za analizu faze sudara postoje dva glavna pristupa u literaturi, zasnovani na održanju energije i održanja impulsa. Zakon održanju impulsa je opisao Brach et all i našli su rešenja za parametre kojima se rekonstruiše sudar. Ovi parametri mogu biti poznati ili se pretpostavljajući koristeći sisteme za praćenje vozila ili fizičke dokaze. U ovom radu je u MATLAB-u formiran model mehanike ravanskog sudara (PIM) zasnovan na metodi najmanjih kvadrata. Baza RICSAC, koja se sastoji od dvanaest realizovanih sudara je korišćena za testiranje modela. Posebna pažnja je posvećena broju parametara koji su usvojeni kao poznati (ili pretpostavljeni). Rezultati ukazuju na važnost svakog parametra.

KLJUČNE REČI: rekonstrukcija saobraćajnih nezgoda, mehanika ravanskog sudara, RICSAC, metoda najmanjih kvadrata, računski model

A COMPUTATIONAL MODEL FOR THE RECONSTRUCTION OF VEHICLE COLLISIONS

Clio G. Vossou, Dimitrios V. Koulocheris

1. INTRODUCTION

Traffic accident reconstruction involves the qualitative and quantitative estimation of the way such an accident occurred. This process includes the use of engineering, scientific and mathematical laws and it is based on data and physical evidence collected from the accident scene.

A typical traffic accident involves the collision of two vehicles and it can be considered in three distinct time phases, the pre-collision, the instantaneous collision and the post-collision phase. In the literature, two broad approaches are used for the simulation of the collision phase, the one based on the conservation of linear and/or angular momentum and the one based on the conservation of energy. The momentum based models are these defined by Brach (Brach, 1987) and Ishikawa (Ishikawa, 1993) while the model considering the conservation of energy is this defined by McHenry (McHenry, 1981).

The momentum based collision simulation model presented by Brach is based on the second law of Newton and the principle of impulse – momentum. This collision model is referenced in the literature as Planar Impact Mechanics model and it consists of six algebraic equations. Since the movement of a vehicle is quantified with three velocity components, the normal, the tangential and the rotational velocity, twelve velocity components, six initial (three per vehicle) and six final ones are involved in this model. Furthermore, this model incorporates three impact coefficients quantifying physical constraints of the collision, namely, the restitution coefficient, the equivalent coefficient of friction and the momentum coefficient of restitution. All fifteen parameters, velocity components and impact coefficients, need to be known, assumed or calculated in order for a traffic accident reconstruction to be accomplished.

In the present paper the Planar Impact Mechanics collision model, which is presented in details in the following section, has been set up in the programming environment of Matlab ®. Planar Impact Mechanics collision model has been coupled with the least squares method in order to calculate the unknown velocity components and/or the impact coefficients. A minimization problem has been set up, using the least squares method equation as a cost function. Using the deterministic optimization method of SQP, implemented in Matlab through the fmincon function, the values of the impact coefficients where determined.

As test cases, the RICSAC database, which consists of twelve staged collisions, has been used. Special attention has been given in the number of velocity components which have been considered known (or assumed) exploring the behaviour of three different cost functions. For the evaluation of the performance of the optimization procedure and the efficiency of each cost function the measured velocity values for each RICSAC test have been used. The results consider the performance of the optimization set up, the performance of each cost function and the importance of the impact parameters.

2. MATERIALS & METHODS

In this section the equations of the Planar Impact Mechanics collision model are going to be introduced. Moreover, the test collisions, belonging in the RICSAC database, are going to be presented. Finally, the least squares method along with the optimization procedure are going to be described providing information on the design variables, the evaluated cost functions and the applicable constraints.

2.1 Planar Impact Mechanics collision model

In 1977 Brach (Brach, 1977) presented a set of six linear algebraic equations which simulate the planar collision of two vehicles. These equations are based on the Newton's second law and the impulse - momentum principles and achieve the calculation of the velocity changes of two particles due to impact (Brach, 1983). This set of equations can be applicable to the simulation of a collision of two vehicles provided that the following assumptions are satisfied (Brach, 1984):

1. The resultant intervehicular impulse is much larger than the impulses of other forces such as friction with the ground, drive train drag and aerodynamic drag which are neglected
2. The resultant impulse vector of the intervehicular force acts at a single point, assumed to be know, called the centre of impact
3. Changes in the position of the centre of mass and in angular orientation in every vehicle are small over the time interval of contact
4. A hypothetical, fixed contact surface is presumed in such a way that motion normal to this surface is due to deformation while motion parallel to this surface has the nature of relative motion corresponding to frictional sliding
5. The time duration of contact is small.

Vehicular collisions typically have contact times less than 0.2 s. Time intervals of this magnitude, coupled with the assumption of large forces cause large accelerations, finite velocity changes and small displacements. All of these considered together, usually, cause the above assumptions to be satisfied for the study of vehicle collisions.

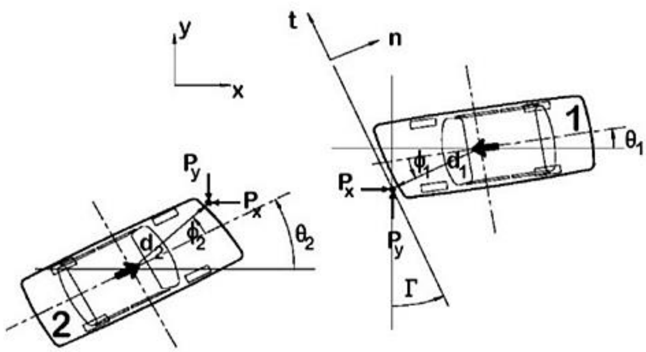

Figure 1. Free body diagram of the collision of two vehicles (Brach, 1983)

In Figure 1, the free body diagram of two vehicles (Vehicle 1 and Vehicle 2) in the collision phase is presented. These vehicles are in contact along the crush surface (line forming angle Γ with y-axis of the global Cartesian Coordinate System (CCS)). Each vehicle has an a priori known mass and inertia, m_i,I_i, respectively. Since the momentum is conserved in each axis of the global CCS Eq. 1 and Eq. 2 are constructed.

$$m_1 \cdot (V_{1fx} - V_{1ix}) + m_2 \cdot (V_{2fx} - V_{2ix}) = 0 \tag{1}$$

$$m_1 \cdot (V_{1fy} - V_{1iy}) + m_2 \cdot (V_{2fy} - V_{2iy}) = 0 \tag{2}$$

he indices 1 and 2 represent each vehicle while the indices i and f stand for the initial (i.e. start of collision phase) and the final (end of collision phase) values, respectively. These indices are used in all following equations.

In Figure 1 the distances d_1 and d_2 correspond to the distance between the centre of mass of each vehicle and the centre of impact. Furthermore, φ_1 and φ_2 represent the angle between d_1 and d_2 and the longitudinal axis of each vehicle while with θ_1 and θ_2 the angle between the the longitudinal axis of each vehicle and the x-axis of the global CCS is denoted. Using these geometrical quantities and the principle of conservation of angular momentum Eq. 3 is derived.

$$I_1 \cdot (\Omega_{1f} - \Omega_{1i}) + I_2 \cdot (\Omega_{2f} - \Omega_{2i}) + m_1 \cdot (d_b + d_d) \cdot (V_{1fy} - V_{1iy}) + m_2 \cdot (d_a + d_c) \cdot (V_{2fx} - V_{2ix}) = 0 \tag{3}$$

In Eq. 3 d_a, d_b, d_c, d_d are correlated to d_1 and d_2 with the following trigonometrical functions.

$$d_a = d_2 \cdot sin(\theta_2 + \varphi_2) \tag{3a}$$

$$d_b = d_2 \cdot cos(\theta_2 + \varphi_2) \tag{3b}$$

$$d_c = d_1 \cdot sin(\theta_1 + \varphi_1) \tag{3c}$$

$$d_d = d_1 \cdot sin(\theta_1 + \varphi_1) \tag{3d}$$

The following three equations (Eq.4 – 6) are provided considering the impact coefficients. The coefficient of restitution, e, is used to model energy loss due to material deformation in a mode normal or perpendicular to the crush surface.

$$\begin{aligned}(V_{1fy} - d_d \cdot \Omega_{1f} - V_{2fy} - d_b \cdot \Omega_{2f}) \cdot sin\Gamma \\ + (V_{1fx} - d_c \cdot \Omega_{1f} - V_{2fx} - d_a \cdot \Omega_{2f}) \cdot cos\Gamma \\ = e \\ \cdot \Big[\Big((V_{1iy} - d_d \cdot \Omega_{1i} - V_{2iy} - d_b \cdot \Omega_{2i}) \cdot sin\Gamma\Big) \\ + (V_{1ix} - d_c \cdot \Omega_{1i} - V_{2ix} - d_a \cdot \Omega_{2i}) \cdot cos\Gamma\Big]\end{aligned} \tag{4}$$

The equivalent friction coefficient, μ, corresponds to the ratio of the tangential to normal impulse components which develop between the vehicles. The tangential impulse is typically attributed to and referred to as friction, though shear deformation is probably equally significant (Brach 1987).

$$m_1 \cdot (V_{1fy} - V_{1iy}) \cdot (cos\Gamma - \mu \cdot sin\Gamma) + m_2 \cdot (V_{2fx} - V_{2ix}) \cdot (sin\Gamma + \mu \cdot cos\Gamma) = 0 \tag{5}$$

Finally, the third coefficient, the moment coefficient of restitution, e_m, governs the rotational effects. A value of this coefficient of unity (1) implies that no moment impulse is developed between the vehicles during collision and that the centre of impact is known. Otherwise any value in the range of [-1, 0] implies that the centre of impact is not known (Barch 1987).

$$\begin{aligned}(\Omega_{1f} - \Omega_{2f}) \cdot (1 - e_m) &= -e_m \cdot \Bigg[\Bigg((\Omega_{1f} - \Omega_{1i}) - m_1 \cdot d_c \cdot \frac{(V_{1fx} - V_{1ix})}{I_1} + m_1 \cdot d_d \cdot \frac{(V_{1fy} - V_{1iy})}{I_1} \\ &\quad - (\Omega_{2f} - \Omega_{2i}) - m_2 \cdot d_a \cdot \frac{(V_{2fx} - V_{2ix})}{I_2} + m_2 \cdot d_b \cdot \frac{(V_{2fy} - V_{2iy})}{I_2}\Bigg)\Bigg]\end{aligned} \tag{6}$$

he Planar Impact Mechanics collision model through the use of these coefficients models the energy loss which is present in all real collisions, since there is loss of kinetic energy, mostly through deformation, friction and vibrational energy. According to the literature (Brach, 1987), typical values of energy loss due to collision range from 25% to 95%.

It is noteworthy that Eq. 1 – 6 correlate (a) six initial velocity components (three for each vehicle – V_{ix}, V_{iy}, Ω_i), (b) six final velocity components (three for each vehicle – V_{fx}, V_{fy}, Ω_f), (c) vehicle inertial properties (I, m) and (d) the collision geometry (d_a, d_b, d_c, d_d, Γ). The aforementioned equations written in a matrix form (Eq. 7) constitute the mathematical collision model (Brach, 1983).

$$A \cdot V_f - C \cdot V_i = 0 \tag{7}$$

2.2 RICSAC database

In the 1970's, while the first computational methods for the simulation of traffic accidents appeared in the literature, the need for a database with fully defined vehicle collisions arose. Within this context a research project named the "Research Input for Computer Simulation of Automobile Collisions" (RICSAC) and funded by the National Highway Traffic Safety Administration (NHTSA), provided the researches with a test matrix of 12 full – scale crash tests. Within this project cameras and accelerometers were attached to the vehicles and a set of staged collision scenarios has been performed resulting into a test matrix of 12 crashes. For each RICSAC test, at least 13 accelerometers were mounted on each vehicle in order to monitor the acceleration components. At three locations, triaxial (XYZ) packages were installed to provide coverage between the front and the rear of the vehicle. The front steer angles were measured on each vehicle by a linear stroke potentiometer attached to the vehicle steering linkage. The time history of the change in vehicle yaw, pitch and roll angles and yaw rate were recorded by two degrees of freedom, free gyroscopes and rate gyro (McHenry, 1987). The final test reports include, also, objective information on the impact speeds, vehicle weights, vehicle dimensions, weight distributions, spin-out trajectories and positions of rest.

RICSAC test database contains vehicle collisions engaging six different vehicles included in four categories of vehicle sizes. The different vehicles used in RICSAC tests are namely (V1) Chevrolet Chevelle, (V2) Ford Pinto, (V3) Ford Torino, (V4) Honda Civic, (V5) VW Rabbit and (V6) Chevrolet Vega. The tests can be classified into four impact configurations (IC1 – IC4) (Figure 2) according to the relative orientation of the vehicles at the time of collision. In the IC1 belong the Tests no. 1, 2, 6 and 7, in the IC2 belong the Tests no. 3, 4 and 5, in IC3 belong the Tests no. 8, 9 and 10 and in IC4 belong the Tests no. 11 and 12. Each crash test involved vehicles of different size categories, except for Test no. 8, which involved two intermediate vehicles. In the front-to-rear collisions (Figure 2b) the car struck in the rear was stopped while in all other tests, both cars were moving.

In the model of structure-borne noise, the engine emission, the properties of its design are integrated into an equivalent cylindrical shell, for which the oscillatory characteristics are known. Equivalence conditions are: equality of mass, length and area of the outer surface of the engine and of such a shell [3].

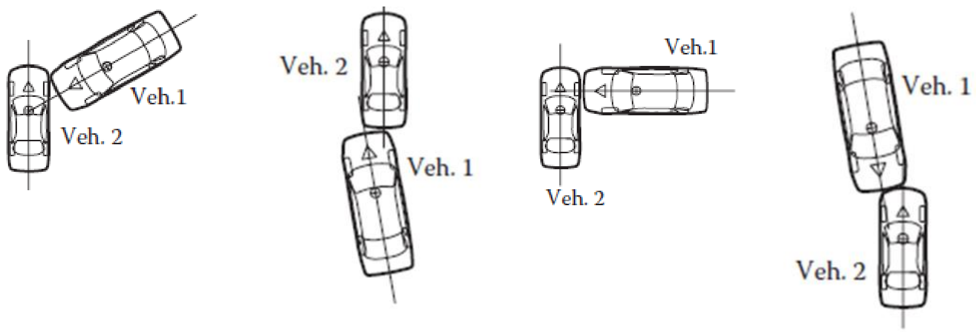

(a) (b) (c) (d)

Figure 2. (a) IC1 - Front corner to corner at 60 o, (b) IC2 - Rear offset oblique at 10 o (c) IC3 - Side perpendicular offset and (d) IC 4 - Frontal offset oblique at 10o (Struble, 2013)

In Table 1, that follows, the measured velocity components of both vehicles for each RICSAC test are presented. This and the following tables are organized per IC and the data of RICSAC test no. 2 are not included due to loss of experimental measurements.

Table 1. Linear and angular velocity for each vehicle for all RICSAC tests

		Impact Configuration (IC)										
		1			2			3			4	
RISAC	Units	1	6	7	8	9	10	3	4	5	11	12
Vi1x	m/s	-8.95	-9.61	-13.01	-9.3	-9.48	-14.89	-9.48	-17.30	-17.75	-9.12	-14.8
Vi1y	m/s	0.00	0.00	0.00	0.00	0.00	0.00	0.00	0.00	0.00	0.00	-4.28
Ωi1	rad/s	0.00	0.00	0.00	0.00	0.00	0.00	0.00	0.00	0.00	0.00	0.00
Vi2x	m/s	4.43	4.66	6.50	0.00	0.00	0.00	0.00	0.00	0.00	8.98	13.87
Vi2y	m/s	7.67	8.32	11.27	9.3	9.48	14.89	0.00	0.00	0.00	-1.58	2.44
Ωi2	rad/s	0.00	0.00	0.00	0.00	0.00	0.00	0.00	0.00	0.00	0.00	0.00
Vf1x	m/s	-3.76	-5.69	-7.74	-3.12	-0.86	-1.55	-5.34	-8.94	-10.46	1.77	4.28
Vf1y	m/s	2.41	1.26	1.48	3.27	4.52	8.59	-0.32	-0.44	0.17	0.62	-0.49
Ωf1	rad/s	-1.57	-0.52	-0.52	-1.99	-3.14	-5.24	-0.42	-0.65	-0.21	0.52	1.57
Vf2x	m/s	-2.07	-1.28	-2.22	-3.66	-3.02	-4.44	-6.73	-9.92	-11.32	1.96	1.93
Vf2y	m/s	5.17	5.49	8.64	6.01	7.38	11.44	1.14	0.42	0.84	-1.26	-2.94
Ωf2	rad/s	0.00	-3.14	-3.35	-0.31	0.79	1.26	-0.42	-0.52	-1.22	0.00	1.05

In Table 2 the geometrical properties of each collision are presented, i.e. the crush angle (Γ) for each IC along with the initial heading angle (θi) and the angle to center of collision (φi). Both angles θi and φi are presented for each vehicle while angle φi is also presented for each RICSAC.

Table 2. Crush angle per RICSAC, initial heading angle and angle to center of collision per vehicle and RICSAC

		Impact Configuration (IC)										
		1			2			3			4	
RISAC	Units	1	6	7	8	9	10	3	4	5	11	12
Γ	deg	-30.0			0.0			-10.0			0.0	
θ1		0.0			0.0			0.0			-10.0	
θ2		60.0			90.0			170.0			0.0	
φ1		-19.8	-17.9	17.9	0.0	6.0	0.0	-17.0	-18.2	-20.7	9.4	9.6
φ2		-38.7	-90.0	-90.0	-68.8	-29.7	-29.2	171.4	171.7	-168.0	11.3	10.3

2.3 Least squares method and minimization problem

As mentioned above, the least squares method is utilized as a means of retrieving a combination of unknown parameters in a way that the equations of the Planar Impact Mechanics model are satisfied and the specified velocity components are closely matched to the estimated ones. The assumed values of the velocity components may result from monitoring devices mounted on the vehicle and/or physical evidence. Such a monitoring device installed in, more vehicles as time progresses, is the Event Data Recorder (EDR). Thus, in the least squares method the velocity components have been included, since an estimate of their value might be available.

In order to utilize the least squares method the vector of all the velocity components included in Eq. 7 is renamed to the vector U in the following way:

$$\{U_1 \quad U_2 \quad U_3 \quad U_4 \quad U_5 \quad U_6 \quad U_7 \quad U_8 \quad U_9 \quad U_{10} \quad U_{11} \quad U_{12}\}^T = \{V_{i1x} \quad V_{i1y} \quad \Omega_{i1} \quad V_{i2x} \quad V_{i2y} \quad \Omega_{i2} \quad V_{f1x} \quad V_{f1y} \quad \Omega_{f1} \quad V_{f2x} \quad V_{f2y} \quad \Omega_{f2}\}^T \tag{8}$$

In order to evaluate the effect of the number of the known and/or estimated velocity components, Eq. 9 – 11 have been set up.

$$Q_1 = \sum_{k=1}^{6} w_k \cdot (U_k - U_k^{est})^2 \tag{9}$$

$$Q_2 = \sum_{k=7}^{12} w_k \cdot (U_k - U_k^{est})^2 \tag{10}$$

$$Q_3 = \sum_{k=1}^{12} w_k \cdot (U_k - U_k^{est})^2 \tag{11}$$

In all three equations w_k, are weighting factors in the range of (0,1] allowing for the definition of different confidence levels for each estimate. In the present paper all w_k have been considered equal to unity stating that all the estimates have the same level of confidence. The experimental estimates U_k^{est} are considered having the corresponding values available in Table 1, i.e. the measured values available in the RICSAC database.

In Q1 (Eq. 9) all the final velocity components have been considered exactly know and their values, equal to those appearing in Table 1, are used in Eq.7. As far as the initial velocity components are concerned, estimates have been considered available, and they were treated as unknowns in Eq.7. On the contrary, in Q2 (Eq. 10), all the initial velocity components have been considered exactly know (Table 1), while experimental estimates have been considered available for the final velocity components. Finally, in Q3 (Eq.11), no velocity component has been considered a priori known, but estimates are considered to exist for all of them. For all three equations, the geometrical properties of the collisions are considered exactly known and having the values appearing in Table 2 while for the impact coefficients (e, μ and em) no experimental values have been considered available.

In order to retrieve the impact coefficients (e, μ and em) these three equations (Eq. 9 – 11) have been coupled with an SQP based optimization subroutine (fmincon) available in Matlab ® in order to achieve the minimization of each Q, forming an equal number of optimization problems.

$$FC_i = \min(Q_i)\, , i = 1 - 3 \tag{12}$$

Each optimization procedure (Eq. 12) provides the values of the design variables, being the three impact coefficients (e, μ and e_m), which minimizes Q_i with U_k values calculated via the least squares method. The Planar Impact Mechanics collision model are included in the optimization procedure in the form of non-linear constraints. Other active constraints of the optimization procedure are the boundary values of the velocity components and these of the design variables. In more details, the linear velocities have been considered in the range of [-20, 20] m/s and the angular velocities have been considered in the range of [-5, 5] rad/s. Respectively, the ranges of the design variables have been considered as: $e \in [0,0.2]$,

$e_m \in [-1,0]$ and $\mu \in [0,1.2]$. The constraints are imported in the optimization procedure through the augmented Lagrange function (L).

3. RESULTS

In the results section the outcome of all three optimization procedures is presented in terms of minimum values of cost function (FCi).

In order to investigate the feasibility of the solution of each minimization procedure along with the value of the cost function, also the values of the derivative of the augmented Lagrange function (∇L) and the vector of the linear constraints (C) are monitored. Moreover, the optimized values of the impact coefficients are introduced and the results regarding the velocity component values are presented in terms of absolute error with respect to the measured, corresponding values. All results are organized per IC and cost function.

In Figure 3 the results of the optimization procedure, for all RICSAC tests, is presented. Each bar represents a different cost function FC_i . It is obvious that FC_2 , which considers the initial velocity components as known quantities provides considerably higher values of cost function in tests 1, 6, 9, 10 and 11. For the rest of RICSAC tests the minimum value of all FC_i is almost the same regardless cost function.

In Table 3, for tests 1, 6, 7, 3, 5 and 11, can be observed that the design variable vector which minimizes FC2 leads to the violation of the constraints. This violation is quantified through the values of the derivative of the augmented Lagrange function (∇L) which has a value significantly greater than 0 in the tests 1, 6, and 11. The value of C is significantly greater than 0 in tests 1, 6, 7, 3 and 5.

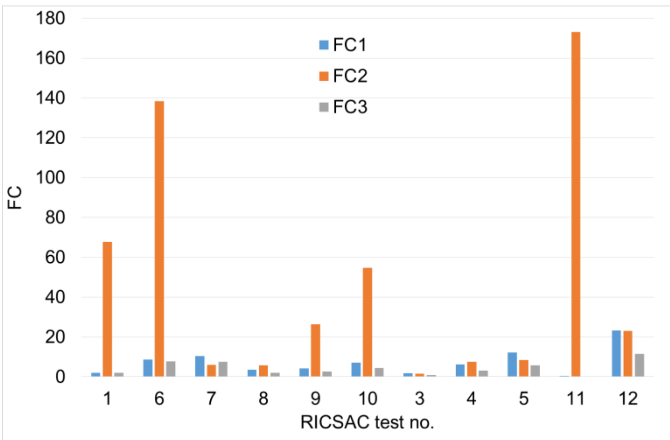

Figure 3. Value of cost function for all cases at the end of the optimization procedure

Table 3. Constraint satisfaction for all optimization problems per RICSAC test

	IC1						**IC2**					
	RICSAC1		**RICSAC6**		**RICSAC7**		**RICSAC8**		**RICSAC9**		**RICSAC10**	
	∇L	**C**	∇L	**C**	∇L	**C**	∇L	**C**	∇L	**C**	∇L	**C**
F1	0.001	0.000	0.000	0.000	0.000	0.000	0.000	0.000	0.000	0.000	0.002	0.002
F2	102.570	0.732	0.122	2.620	0.000	2.830	0.000	0.000	0.000	0.000	0.000	0.003
F3	0.001	0.000	0.002	0.000	0.000	0.000	0.000	0.000	0.001	0.000	0.002	0.000

	IC3						**IC4**			
	RICSAC3		**RICSAC4**		**RICSAC5**		**RICSAC11**		**RICSAC12**	
	∇L	**C**	∇L	**C**	∇L	**C**	∇L	**C**	∇L	**C**
F1	0.000	0.000	0.001	0.000	0.000	0.000	0.001	0.000	0.000	0.000
F2	0.005	0.260	0.003	0.000	0.000	1.010	23.060	0.003	0.004	0.001
F3	0.001	0.000	0.000	0.000	0.001	0.000	0.000	0.000	0.001	0.000

In the following Tables 4, 5 and 6 the absolute error values for each velocity component and every RICSAC test for all three cost functions (FC_1 – FC_3) are presented.

Table 4. Absolute error for all velocity components in m/s for each vehicle for all RICSAC tests for the cost function FC_1

		Impact Configuration (IC)										
		1			**2**			**3**			**4**	
	RISAC	**1**	**6**	**7**	**8**	**9**	**10**	**3**	**4**	**5**	**11**	**12**
Absolute error	**Vf1x**	0.25	-0.61	-1.18	1.07	1.01	1.50	0.08	1.63	1.13	0.10	-0.18
	Vf1y	-1.23	-0.47	-0.85	-0.22	0.76	0.33	0.40	0.52	0.92	-0.07	0.99
	Ωf1	0.35	1.52	2.17	0.13	-1.44	-1.13	0.36	0.86	1.01	0.17	-0.97
	Vf2x	0.94	1.48	0.38	1.20	0.49	1.35	-0.29	0.57	-0.12	0.13	-0.68
	Vf2y	0.71	1.53	1.75	0.39	-0.33	-0.61	0.00	1.07	1.13	0.67	-2.44
	Ωf2	0.84	-1.10	-0.66	0.90	-0.41	-1.09	0.36	0.99	0.00	0.17	0.21

Table 5. Absolute error for all velocity components in m/s for each vehicle for all RICSAC tests for the cost function FC_2

		Impact Configuration (IC)										
		1			**2**			**3**			**4**	
	RISAC	**1**	**6**	**7**	**8**	**9**	**10**	**3**	**4**	**5**	**11**	**12**
Absolute error	**Vi1x**	-4.16	-5.56	0.34	-1.00	2.43	4.71	0.10	-1.68	-1.07	-7.25	-0.16
	Vi1y	2.07	1.79	0.48	0.03	2.25	1.86	0.84	0.68	1.21	0.62	-0.99
	Ωi1	2.67	1.68	1.79	0.42	3.15	2.78	0.79	0.30	2.06	1.11	1.98
	Vi2x	-3.92	-0.68	-0.81	1.27	2.07	4.38	0.08	0.49	0.01	-7.09	0.69
	Vi2y	-2.00	-3.69	-1.21	-0.15	1.01	1.36	0.08	1.32	1.06	-0.32	-1.44
	Ωi2	3.24	3.61	0.65	1.73	0.46	0.49	0.79	1.49	0.61	0.06	2.41

Table 6. Absolute error for all velocity components in m/s for each vehicle for all RICSAC tests for the cost function FC_3

		Impact Configuration (IC)										
		1			2			3			4	
	RISAC	**1**	**6**	**7**	**8**	**9**	**10**	**3**	**4**	**5**	**11**	**12**
Absolute error	**Vi1x**	-0.34	-0.33	0.13	-0.53	-0.25	-0.36	0.03	-0.81	-0.56	0.03	-0.09
	Vi1y	0.47	0.14	0.14	0.09	0.45	0.24	0.41	0.25	0.63	0.03	-0.49
	Ωi1	0.44	0.39	1.07	0.15	0.46	0.35	0.45	0.60	1.30	0.08	0.89
	Vi2x	0.23	0.09	-0.29	0.61	0.39	0.95	0.11	0.29	0.04	-0.08	0.34
	Vi2y	-0.20	-0.37	-0.57	-0.18	0.20	0.34	0.02	0.53	0.57	-0.33	-1.71
	Ωi2	0.47	0.19	0.20	0.39	0.22	0.01	0.23	0.30	0.38	0.08	1.32
	Vf1x	-0.02	-0.86	-1.00	0.53	0.38	0.69	0.00	0.81	0.56	0.06	-0.09
	Vf1y	-0.68	-0.54	-0.64	-0.09	0.45	0.24	0.00	0.25	0.29	-0.03	0.49
	Ωf1	-0.05	1.23	1.39	-0.08	-1.10	-0.92	0.00	0.38	-0.08	0.09	-1.11
	Vf2x	0.60	1.27	0.58	0.59	0.27	0.62	0.00	0.29	-0.04	0.06	-0.34
	Vf2y	0.41	1.06	1.08	0.18	-0.20	-1.06	0.00	0.53	0.57	0.33	-1.71
	Ωf2	0.45	-1.39	-1.06	0.61	-0.61	-1.07	0.00	0.51	-1.09	0.08	-1.00

The maximum absolute error for the use of cost function FC_1 is -2.44 m/s and it appears in RICSAC test 12 in the velocity component Vf2y. If FC_2 is used then the maximum absolute error is -7.25 m/s and it appears in RICSAC 11 in the Vi1x. Finally, the maximum absolute error using FC_3 is -1.71 m/s and it appears again in RICSAC 11 in the velocity component Vi2y. In Figure 4 the values of the impact coefficients are presented in the form of bar diagrams. For all impact coefficients, the vertical axis represent the applicable range of values while the horizontal axis is organized per RICSAC test. The different color in bars indicates use of different cost function, FC_i. Lack of a bar indicates that using the corresponding cost function FC_i the optimization procedure converges for the minimum value of this impact coefficient. In RICSAC tests 9, 10 and 3 the coefficient of restitution (Figure 4a) reached its maximum allowable value regardless cost function. In the rest of the tests every cost function provides different value for the coefficient of restitution. In all RICSAC tests, except RICSAC 5 FC_2 provides the lowest value of coefficient of restitution. Furthermore, FC_3 provides higher value for the coefficient of restitution compared to FC_1 with the exception of RICSAC 5. The value of the moment coefficient of restitution (Figure 4b) is more uniform. In all RICSAC tests except 1, 7, 4 and 11 all cost functions provide the same value for this coefficient which is either its lower (6, 3, 5) or its upper bound (8, 9, 10, 12). As far as the values of the equivalent coefficient of friction (Figure 4c) is concerned they show significant non-uniformity. Nevertheless in RICSAC tests belonging to IC1, FC_2 seems to provide the highest values, followed by FC3. In RICSAC tests 9 and 10 the opposite seems to happen, while in tests 3, 5 and 12 all cost functions provide the same value of friction coefficient.

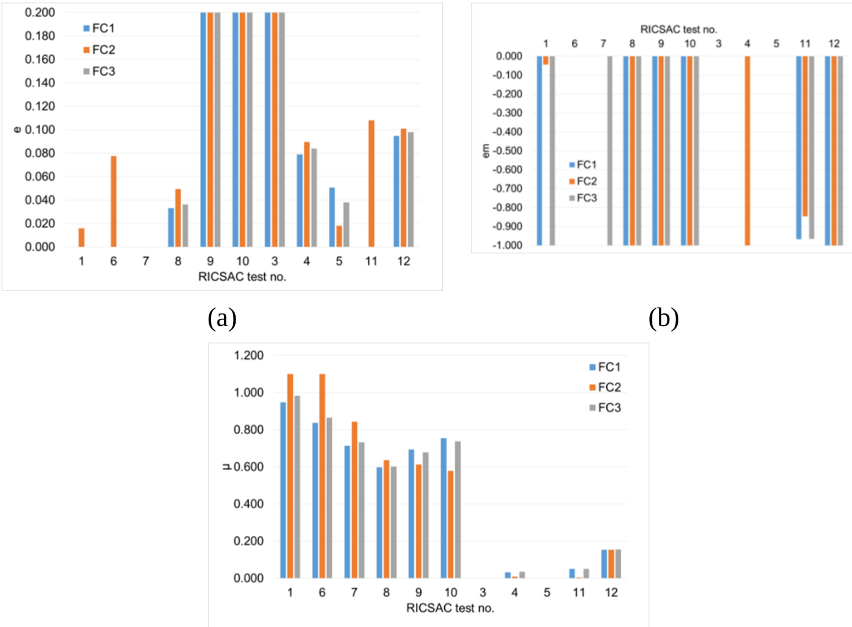

(a) (b)

(c)

Figure 4. Optimized value of the (a) restitution coefficient e, (b) moment coefficient of restitution em and (c) coefficient of friction μ for all RICSAC and all cost functions

4. DISCUSSION

In Figure 3 is obvious that FC_3 provides the overall minimum value for all RICSAC tests, while FC_2 provides the highest value in most RICSAC tests. The fact that FC_3 provides results of better quality is also obvious in Table 6 where the absolute error for all velocity components are presented. In Table 3 where the values of ∇L and C are presented, is obvious that FC_2 leads to violation of the constraints in tests 1, 6, 7, 3, 5 and 11, meaning that Eq. 7 is not satisfied, i.e. these solution vectors cannot be taken under consideration.

In order to quantify, in more details, the quality of each solution the error of the change of velocity in every vehicle is also considered. The components of the vehicle's change of velocity (ΔV_i) were computed by subtracting the initial velocity at impact from the velocity at the time of separation. The procedure was performed for the X and Y velocity component separately. The measured change in velocity ΔV is provided in the literature (Brach, 1982) as an overall measure of the severity of a collision. In Table 7 the measured velocity changes are presented per IC and RICASC test.

In Figure 5 the relative computed velocity changes are presented for Vehicle 1 (Figure 5a) and Vehicle 2 (Figure 5b) for the cost functions FC_1 and FC_3. The relative computed velocity change was calculated as the difference between the measured and the computed velocity change divided by the measured one. FC2 was omitted for Figure 5 since, as it was discussed earlier, it leads to solution vectors that may violate both the linear and the non-linear constraints.

The accuracy of both cost functions as far as the velocity change is concerned is fairly good. The relative computed velocity change ranges from 0 to 25% for FC_1 and from 0 to 36% for FC_3. The maximum value of relative computed velocity change appears for both cost functions in RICSAC test 10 and Vehicle 2. In general, the values of the relative computed velocity change are larger in Vehicle 2 where 36% is met, than in Vehicle 1. The highest value Vehicle 1 is 19%.

Table 7. Absolute measured ΔV for each vehicle and RICSAC test

IC1	**RICSAC**	**1**		**6**		**7**	
	Vehicle	**1**	**2**	**1**	**2**	**1**	**2**
	Measured ΔV (m/s)	5.72	6.96	4.12	6.58	5.47	9.11
IC2	**RICSAC**	**8**		**9**		**10**	
	Vehicle	**1**	**2**	**1**	**2**	**1**	**2**
	Measured ΔV (m/s)	6.99	4.92	9.73	3.68	15.87	5.81
IC3	**RICSAC**	**3**		**4**		**5**	
	Vehicle	**1**	**2**	**1**	**2**	**1**	**2**
	Measured ΔV (m/s)	4.15	6.83	8.37	9.93	7.29	11.35
IC4	**RICSAC**	**11**		**12**			
	Vehicle	**1**	**2**	**1**	**2**		
	Measured ΔV (m/s)	10.91	7.03	18.75	13.10		

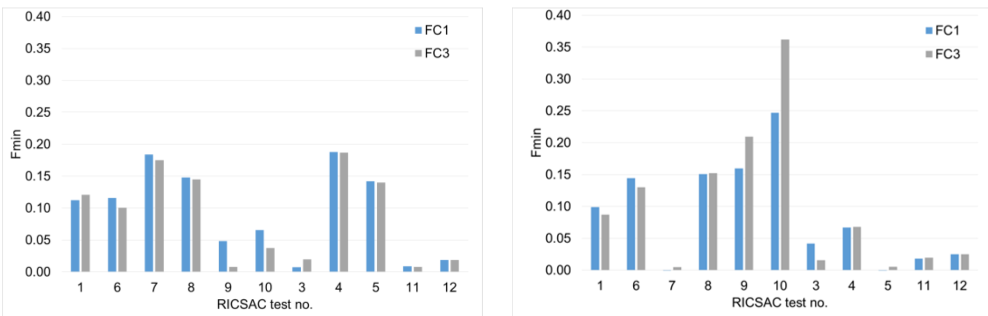

(a) (b)

Figure 5. Relative velocity change for cost functions 1 and 3 for vehicle (a) 1 and (b) 2

As far as the impact coefficients are concerned, in Figure 4, is obvious that only equivalent friction coefficient depends on the cost function used. Both the restitution coefficient, and the moment coefficient of restitution demonstrate a dependence on the test conditions. Furthermore, the moment coefficient of restitution in most tests obtains one of its boundary values.

5. CONCLUSIONS

In the present paper the Planar Impact Mechanics collision model has been implemented in Matlab® and coupled with the least squares method. Three different cost functions based on least squares method have been minimized with the deterministic optimization method of SQP in order to calculate the velocity components of two vehicles in collision and provide the impact coefficients which verify the PIM collision model. The presented methodology is a way to utilize EDR data (Brach, 2011). Comparing three scenarios through different cost functions it was indicated that the most reliable results where produced when estimates for all velocity components were available (FC3).

The values of absolute error of the velocity components are comparable for all RICSAC tests and all cost functions, but are quite high. It is worth mentioning that a concern has risen in the past, with respect to the accuracy of the velocity components documented in RICSAC reports. In 1997 a re-evaluation of the provided data has been proposed, since it was realized that the measuring devices were not placed on the centre of mass of each vehicle (McHenry and McHenry, 1997). Furthermore, in the reports of the RICSAC tests (Jones, 1978) it is acknowledged that the value of the separation velocity in all tests was contaminated by the effects of rotation of the vehicles between impact and separation. The abovementioned facts influence the performed analysis within this study, in terms of relative values, since the re-evaluated values have not been taken under consideration. Finally, as far as the impact coefficients are concerned, they were successfully computed regardless cost function, with slight differences in most RICSAC tests for both the moment coefficient of restitution and the coefficient of restitution. On the other hand each cost function leads to a different value for the friction coefficient, leading to the conclusion that this is the more decisive impact coefficient.

REFERENCES

[1] Ishikawa, H.: "Impact model for accident reconstruction-normal and tangential restitution coefficients", (No. 930654) ", SAE Technical Paper, 1993.

[2] Brach, R., Brach, R.: "A review of impact models for vehicle collision", SAE Technical Paper, No. 870048, 1987.

[3] McHenry, R,: “CRASH3 Users Guide and Technical Manual” NHTSA, DOT Report HS, 805, 732, 1981.

[4] Brach, R.: “Least Squares Collision Reconstruction”, SAE Technical Paper, No. 870429, 1987.

[5] Brach, R.: "An impact moment coefficient for vehicle collision analysis", SAE Transactions, 1977, pp 30-37.

[6] Brach, R.: "Identification of vehicle and collision impact parameters from crash tests", Journal of vibration, acoustics, stress, and reliability in design, Vol. 106, No. 2, 1984, pp 263-269.

[7] Brach, R.: "Momentum and Energy Analysis of Automobile Collisions", Trans. Structural Impact and Crashworthiness, Elsevier Appl. Sci. Publ, 1984.

[8] Brach, R.: "Nonlinear Parameter Estimation of a Vehicle Collision Model", 13th Annual conference on Modeling and Simulation, University of Pittsburgh, April 1982.

[9] McHenry, B., McHenry, R.: "RICSAC-97 A Re-evaluation of the Reference Set of Full Scale Crash Tests”, SAE Technical Paper, No. 970961, 1997.

[10] Jones, I., Baum, A.: "Research Input for Computer Simulation of Automobile Collisions, Volume IV: Staged Collision Reconstructions", DOT HS-805, 40, 1978.

[11] Struble, D.: "Automotive accident reconstruction: practices and principles", CRC Press, 2013.

MOBILITY & VEHICLE MECHANICS

DOI: 10.24874/mvm.2018.44.03.04
UDC: 614.862

AUTOMOTIVE SAFETY CONTROL SYSTEM BASED ON TIMEAXIS DESIGN

Satoru Furugori [1], Takeo Kato [2], Yoshiyuki Matsuoka [3]*

Received in July 2018 Accepted in August 2018

RESEARCH ARTICLE

ABSTRACT: Timeaxis design is a design concept that incorporates the concept of time axis into design theory and methodology. Under this design framework, different methods, such as models those who integrate multiple timescales, those employ identity mapping to describe non-linear and non-steady phenomena and those employ genetic network programing to describe phenomena evolving gradually as times pass, have been proposed. We applied Timeaxis design to develop an automotive safety control system that considers risks at a short timescale (second/minute), medium timescale (hour/day), and long timescale (month/year). This system displays the driving state on the basis of the state of the driver's vehicle, surrounding vehicles, and driver's physical conditions, generates the vehicle control algorithm on the basis of the driver's state, and provides driving advice to the driver in real time. With this system, it is possible to correspond to future safety issues such as problems caused by mixing of autonomous vehicles and conventional vehicles, problems caused by reduction in driving skill due to automation of driving and problems caused by the decline in driving ability with aging.

[1]*Satoru Furugori, Ph.D., Assoc. prof., Keio University, Graduate School of Science and Technology, 3-14-1, Hiyoshi Kohoku-ku Yokohama 223-8522, Japan, furusa212@gmail.com*
*(*Corresponding author)*
[2]*Takeo Kato, Ph.D.,assist. prof., Keio University, Department of Mechanical Engineering, -14-1 Hiyoshi Kohoku-ku Yokohama 223-8522, Japan, kato@mech.keio.ac.jp*
[3]*Yoshiyuki Matsuoka, Ph.D. prof.., Keio University, Department of Mechanical Engineering, -14-1 Hiyoshi Kohoku-ku Yokohama 223-8522, Japan, matsuoka@mech.keio.ac.jp*

KEY WORDS: timeaxis design, multi-timescale model, identity mapping model, genetic network programming, automotive safety control system

UPRAVLJANJE SISTEMIMA BEZBEDNOSTI VOZILA ZASNOVAN NA INTERVALU VREMENA U PROJEKTOVANJU

REZIME: Interval vremena u projektovanju je koncept projektovanja koji uključuje koncept intervala vremena u teoriju projektovanja i metodologiju. Ovakva struktura projekta obuhvata različite metode, ako što su modeli koji integrišu višestruke vremenske skale, primenjuju mapiranje identiteta koji opisuju nelinearne i nestacionarne fenomene i one koji obuhvataju genetičke mreže za programiranje kako bi opisali fenomene koji evoluiraju kako vreme prolazi. Primenili smo koncept intervala vremena u projektovanju da bismo razvili upravljanje sistemom bezbednosti vozila koji uzima u obzir rizike u kratkom vremenskom intervalu (sekund/minut), srednjem vremenskom intervalu (sat/dan) i u dugom vremenskom intervalu (mesec/godina). Ovaj sistem prikazuje stanje vožnje na osnovu stanja vozača vozila, okolnih vozila, i fizičkih uslova okruženja vozača, pri čemu generiše algoritam upravljanja vozilom na osnovu stanja vozača i daje savete vozaču u realnom vremenu. Sa ovim sistemom je moguće dati odgovore u budućnosti koji se odnose na probleme bezbednosti nastali kao posledica istovremenog delovanja autonomnih i konvencionalnih vozila, problema izazvanih redukovanom veštinom vožnje usled automatizacije vožnje i problema izazvanih starenjem koji ograničavaju sposobnost vožnje.

KLJUČNE REČI: interval vremena u projektovanju, model višestrukog vremena, model mapiranja identiteta, programiranje genetske mreže, upravljanje sistemom bezbednosti

AUTOMOTIVE SAFETY CONTROL SYSTEM BASED ON TIMEAXIS DESIGN

Satoru Furugori, Takeo Kato, Yoshiyuki Matsuoka

1. INTRODUCTION

To support the maintenance of the global environment and the sustainable development of the society and economy, the theory and methodology of Timeaxis design has been proposed [1-3]. Under this framework, changes in different factors operating along different time axes are considered, including different circumstances and a "sense of value" such as interest in driving are incorporated into design. With respect to the automobile traffic, it is necessary to explore means of transportation that cause less traffic accidents, are moved efficiently, and generate with fewer CO2 emissions and less environmental pollution. Hurried driving may increase the probability of accidents, while too much focus on safety increases travel time, CO2 emissions, and environmental pollution. Therefore, safety, efficiency, CO2 emissions, and the environmental burden of vehicles are in a relation of the trade-off each other; the prioritization of these factors depends on the individual's purpose of the movement and on traffic conditions. However, individual drivers cannot judge whether their driving is appropriate given the situation and circumstances. Therefore, this study aims to propose a new automotive safety control system having the following three functions: 1) the vehicle itself objectively displays its current state; 2) the vehicle changes its control to adapt to the requirement of individual drivers; 3) the vehicle advises appropriate driving in the situation and circumstances. These functions enable safer driving with minimal environmental impact. In conventional automobile development, the technologies for CO2 reduction (e.g., hybrid vehicles and engines with high fuel economy), safety (e.g., safety support systems and autonomous vehicles), efficiency (e.g., traffic signal controls and vehicle platooning) and reducing the environmental burden (e.g., electric vehicles and fuel cell vehicles) have been individually developed. Each technology has been developed with the goal of clearing standards measured with fixed modes such as safety and CO_2 emission, and it is not necessary to consider the trade-off between technologies to acquire the certification. Therefore, no technical framework for optimizing the automotive control in use situations has been studied. However, there is no technical framework for overall optimization given the purpose of personal movement, so a driver cannot know whether or not his or her type of driving is appropriate given the situation. Accordingly, it is impossible to know whether the vehicle is appropriately controlled in the situation and circumstances and whether the driver is performing appropriate driving behaviour for the vehicle control. In this paper, a framework for an automotive safety control system is proposed based on the theory and methodology of Timeaxis design. In this system, the vehicle displays its current driving state, and the vehicle switches its means of control according to the driving state while advising the driver on how to safely drive and on how to lessen the environmental burden.

2. MODEL USED FOR TIMEAXIS DESIGN

Timeaxis design is a theory and methodology that incorporates the concept of time axes into design. Explicit manipulation of time axes cannot be accomplished in conventional optimization methods and systems engineering, and, so far, design theory has not actively addressed the concept of “time axes.” In some cases, designers have assumed that time axes change the use stage (as a minor consideration), but design principles have not been explicitly based on this concept. For this reason, it is not possible to intentionally or effectively respond to changes in the time axes of circumstances, such as variations in usage environments or type of use. In Timeaxis design, several models are used to incorporate phenomena operating along distinct time axes. At following, we explain the three Timeaxis design models that we incorporated into the framework of our proposed automotive safety control system.

2.1 Non-steady model

A non-steady model describes elements of non-steady phenomena and their relationships. Many phenomena during driving are non-steady. Vehicles are equipped with various sensors, and vehicle data such as speed, accelerator operation, brake operation, steering wheel operation, etc., are measured in real time. The vehicle data obtained from sensors are non-steady because roads such as expressways, urban roads, winding roads, etc., change irregularly, and conditions of congestion also irregularly vary. Also, it may be necessary to arrive early, for example, or to change the type of driving. The type of driving may additionally change because of changes in physical conditions. Furthermore, there is the possibility of encountering an unexpected, non-steady state, such as a traffic accident. Therefore, a non-steady model is necessary to objectively indicate the state in which a vehicle is currently in. As an example of a non-steady model, we examined a framework to describe driving states using an identity mapping model, as shown in Figure 1 [4-7]. The identity mapping model is a hierarchical network model in which the number of input and output layers is the same and the number of units in the intermediate layer is smaller than the number of units in the input and output layers. In the identity mapping model, learning is performed such that the input signals and the output signals are equal. The features of the input layer are expressed as the output of the intermediate layer, which contains fewer features than the input layer. By mapping and displaying the intermediate layer, it is possible to monitor the time changes of non-steady phenomena.

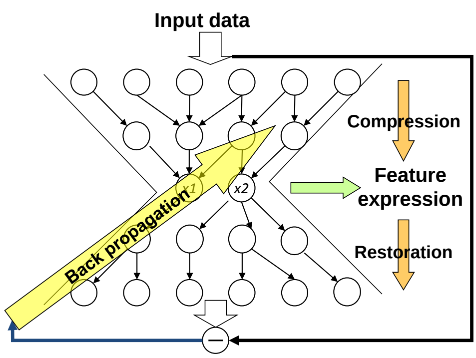

Figure 1. Example of a non-steady model (identity mapping model)

2.2 Plasticity model

A plasticity model describes properties such as gradually changing structures and functions with respect to time axes. Driving a vehicle entails plastic phenomena including, for example, the improvement of driving ability or driving skills to generate fewer CO2 emissions. In the plasticity model, such changes are described based on past driving ability, and it does not return to the past state. As an example of a plasticity model, we used a framework to generate engine control algorithms according to changes in driving states based on genetic network programming (GNP), which is an evolutionary computation, as shown in Figure 2 [8-10]. In nature, organisms change genetic information by selection, crossover, mutation, etc., and adapt to the surrounding environment. Genetic algorithms (GAs) apply the evolutionary processes of organisms to express genetic information using a bit array structure that considers genetic manipulation. GNP is an extension of GAs and is based on the representation of a gene using a network structure instead of a bit array. As evolution progresses, the connection state gradually changes so as to maximize the objective function.

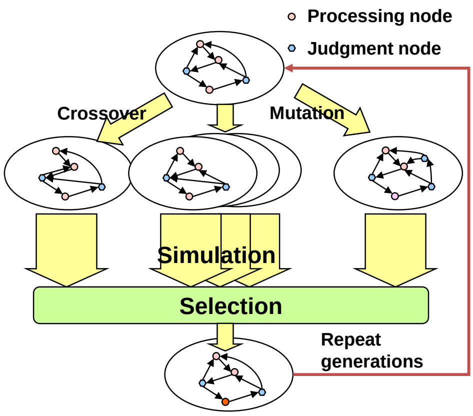

Figure 2. Example of a plasticity model (genetic network programming)

2.3 Multi-timescale model

The multi-timescale model describes the experience of multiple time axes at the same time. A driver instantaneously controls a vehicle so as not to collide with surrounding vehicles and may also perform driving considering daily CO_2 emissions. In addition, current driving behaviour may change as a result of the development of driving skills or long-term changes in driving skills. Therefore, current driving behaviour is considered to be the result of combining these controls. As shown in Figure 3, the multi-timescale model is based on the integration of different timescales. In addition, the multi-timescale model considers a hierarchy of time-axis scales, wherein the short timescale corresponds with seconds or minutes, the medium timescale with hours or days, and the long timescale with months or years. This model is effective for designing each timescale and for integrating the design of timescales by considering their relationships.

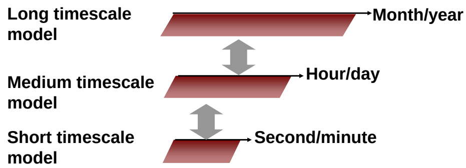

Figure 3. Example of a multi-timescale model

3. APPLICATION OF TIMEAXIS DESIGN TO THE AUTOMOTIVE SAFETY CONTROL SYSTEM

The automotive safety control system proposed in this paper is aimed to provide future transportation for society by around 2030. In this future transportation society, autonomous vehicles and manual conventional vehicles will coexist. Electric vehicles, hybrid vehicles, and internal combustion locomotives will also be mixed. Vehicles equipped with the proposed system will change controls according to the desires of individual drivers, such as safe driving, good fuel economy, or low electricity cost-based driver's driving history. For drivers who feel a sense of burden in driving, autonomous driving can be set as the dominant control. Meanwhile, drivers who want to enjoy driving or to improve driving skill can be given responsive engine control. Furthermore, driving advice can be provided according to individual driving characteristics. The proposed system can be installed in vehicles as a core module. Next, the three functions of the core module will be described using analysis data. The driving data used for this analysis were taken in 300 seconds at intervals of 0.1 seconds using a driving simulator. The data were used once for model learning and 10 times for verification.

3.1 Driving state display based on identity mapping model

The driving state display is a function that instantaneously grasps current driving conditions, including approaching dangers to the vehicle, etc., at the moment that a driver is operating a vehicle. To instantaneously display the driving state in an easy-to-understand manner, it is necessary to compress the driving data measured by many vehicle parameters and to display features with only a small number of parameters. Therefore, the identity mapping model for compressing non-steady data was used to extract features from the driving data. Figure 4 shows the driving state extracted from features. The inputs for the vehicle parameters are vehicle speed and its differential, inter-vehicle distance and its differential, and brake pedal angle and its differential. The number of intermediate layers was set to 2, and the resulting map was displayed. Here, based on the relative relationship with the preceding vehicle, the driving state was classified into "collision," "proximity," "approach," "leave," follow," and "free." As time elapses, the driving state value moves within this map; the same driving states are located within the same vicinity. Several boundaries were described as straight lines, which classify several driving states. In this example, the features of the driving state with respect to the distance to the preceding vehicle are shown, but it is also possible to display the state of the behavior of the vehicle itself and the risk state of the driver at the same time. Thus, a framework for understanding the driving state based on a two-dimensional map was constructed.

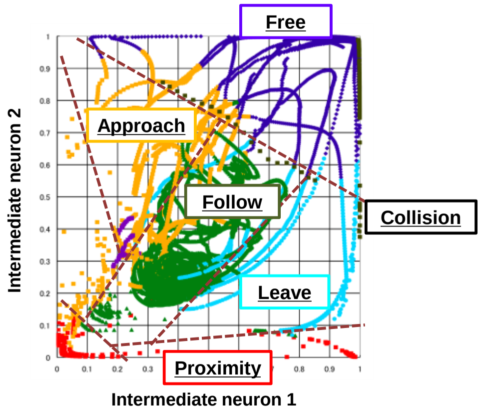

Figure 4. Mapping of the driving state based on an identity mapping model

3.2 Vehicle control based on genetic network programming

This vehicle control is a function oriented toward safe, fuel-efficient, and environmentally friendly driving by switching to a vehicle control that is adapted to individual driving and based on the current driving state. There is a possibility that the instantaneously acquired driving data may indicate a driving state that has never been experienced. In such a case, it is necessary to create a new vehicle control algorithm. So, GNP was used to create a new vehicle control algorithm. Figure 5 shows an example of the vehicle control algorithm that emerged. GNP derived an optimal engine control algorithm that minimizes travel costs (fuel and battery costs) when new driving states, such as flat roads, ascending roads, descending roads, or congested roads, are detected, and it was confirmed that the travel cost was reduced by switching between these control algorithms. Thus, a framework of vehicle control was constructed that is created for driving states where no control logic is available. In this scenario, a new control algorithm emerges, and the vehicle control switches to the optimal algorithm.

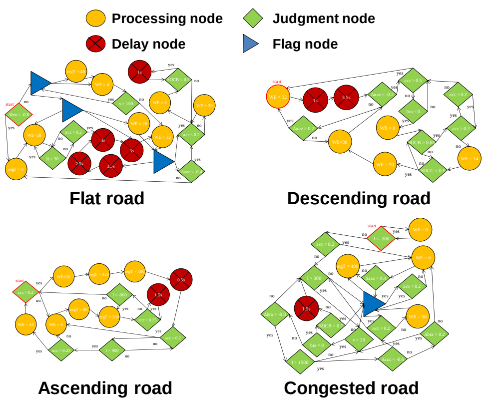

Figure 5. Development of the engine control algorithm and switching

3.3 Timing of advice based on changes in driving state

Driving advice is presented at the time when the driving state changes and is associated with vehicle behaviour. Figure 6 shows an example wherein the timing of driving advice is displayed on a map of inter-vehicle distance and relative speed. As the vehicle moves, the driving state value moves on the map and crosses the boundary lines that dictate the timing of advice. The position of the boundary lines varies depending on the individual driver, and knowledge is acquired via learning from driving data. Ultimately, the boundary lines of the driving state display shown in Figure 4 indicate the timing of advice.

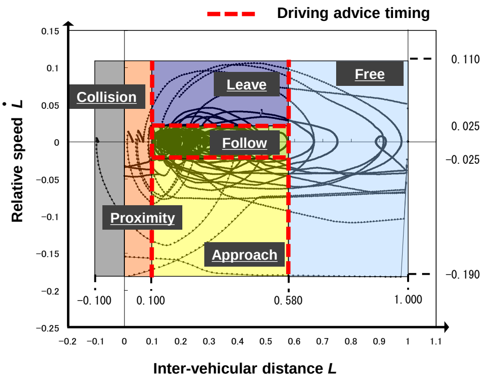

Figure 6. Setting of advice timing for the driver

4. FRAMEWORK FOR PROPOSED AUTOMOTIVE SAFETY CONTROL SYSTEM

The three functions described in the previous chapter were integrated using a multi-timescale model. Figure 7 shows the framework of the proposed vehicle safety control system. At the short timescale, the real-time display of the driving state, the vehicle control, and the notification of driving advice to the driver at a set time are performed. First, the driving state is estimated and displayed based on vehicle data and data from the surrounding environment. When the running state is known, the corresponding control algorithm is selected to control the vehicle. Furthermore, advice is given to the driver at a set time. If the driving state is unknown, an approximate driving state is searched for, passing the vehicle data and the surrounding environment data to the middle timescale while continuing to display the control and advice in real time. At the middle timescale, a control algorithm corresponding to an unknown driving state is developed. Next, the vehicle data, the surrounding environment data, and the control algorithm are passed along to the long timescale. At this scale, the driver's desires with respect to the level of safety and the cost of travel are estimated, generating advice so that the driver's behavior changes to meet his or her desires based on the analysis of long-term records of the driving state.

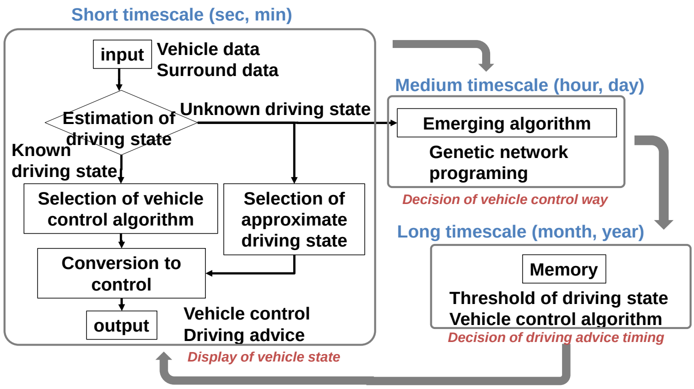

Figure 7. Framework of the vehicle safety control system based on a multi-timescale model

5. DISCUSSION

Issues that are important for transportation in future society were considered in the vehicle control system proposed herein. These issues include risk resulting from the mixture of conventional vehicles and autonomous vehicles, risk resulting from the decline in driving skills following the introduction of autonomous driving, and risk resulting from the decline in driving ability with aging. Regarding the first risk, the proposed system will be able to distinguish whether a vehicle is autonomous or conventional by learning the features of the type of driving. An autonomous vehicle may obstruct smooth traffic to comply with traffic rules and increase the safety margin. When such a vehicle is encountered, smooth and safe driving can be achieved based on driver judgment of whether to interrupt the control and, for example, move ahead of another vehicle or give the right-of-way. Regarding the second risk, the proposed system is designed to improve according to an individual's growth regardless of whether a driver prefers autonomous driving or wishes to improve his or her skill and enjoys driving. Therefore, the vehicle control and driving advice will change according to an individual's growth, compensating for decline in driving skill as well. Regarding the third risk, the proposed system considers the life cycle of a vehicle from purchase until disposal as well as past travel history, which can be transferred to a new vehicle. Upon accumulating driving history from a beginning point in time until a latter point in time as a driver ages, it is possible to cope with changes in driving ability due to aging. One future task for completing the automotive safety control system is the consideration of an algorithm for automatically changing the boundary of the driving state with respect to the driving state display based on the identity mapping model. Also, in accordance with the growth of individuals, it is necessary to develop artificial intelligence (AI) that can judge the type of driving that a driver is oriented toward.

6. CONCLUSIONS

We applied the theory and methodology of Timeaxis design to propose a framework for an automotive safety control system that may be placed into effect around 2030. The proposed system consists of a display of the driving state, algorithms for determining vehicle control, and functions for providing driving advice. The use of a framework based on a multi-timescale model consisting of a short timescale, medium timescale, and long timescale enables trade-off between problems at different scales, such as efficiency and safety.

Furthermore, by designing the system as a core module to be mounted on the vehicle, even when changing the vehicle, the past travel history so far is taken over by switching the core module. As a result, it is possible to make safety control and driving advice in consideration of long-term changes such as a change in driving ability due to aging. In addition, since the system is designed to improve according to individual's growth, it is not necessary for the manufacturer to add both the autonomous vehicle and the safety support vehicle to the product line up. Manufacturers need to provide a common architecture of safety vehicles that combines both functions and changes with learning.

ACKNOWLEDGMENTS

I appreciate the support from Keio University research scholarship.

REFERENCES

[1] Matsuoka, Y.: "Design Science for Product Creation X Product Usage", Kindai-Kagaku-Sha, 2017, pp. 43–55.

[2] Arita, M., Kikuchi, M., Kato, T., Hui, P., Matsumoto, A., Sato, K., Kato, T., Matsuoka, Y.: "Development of Basic Architecture for Health Monitoring Seat System", Journal of the Science of Design, Vol. 1, No. 2, 2017, pp. 71-80.

[3] Kamiya, K., Kito, A., Alvarez, J., Sato, K., Nishimura, H., Matsuoka, Y., Furugori, S.: "Timeaxis Design of a Service System Growing Values of Mobility Using the M-V Model", Design, User Experience, and Usability. Experience Design for Everyday Life Applications and Services, Third International Conference, DUXU 2014, Heraklion, Crete, Greece, June 22-27, 2014, pp. 281–292.

[4] Chalodhorn, R., MacDorman, K, Asada, M.: "Humanoid Robot Motion Recognition and Reproduction", Advanced Robotics, Vol. 23, No. 3, 2009, pp 349-366.

[5] Kramer, M.: "Nonlinear Principal Component Analysis Using Autoassociative Neural Networks", AIChE Journal, Vol. 37, No. 2, February 1991, pp. 233–243.

[6] Cottrell, G., Munro, P., Zipser, D.: "Image Compression by Back Propagation: An Example of Extensional Programming", Advances in Cognitive Science, Vol. 3, 1988, pp. 208-240.

[7] Yoshimura, H., Shimizu, T., Isu, N., Sugata, K.: "Construction of Noise Reduction Filter by Use of Sandglass-Type Neural Network", IEICE Trans. Fundamentals, Vol. E80-A, No. 8, August 1997, pp. 1384-1390.

[8] Mabu, S., Hirasawa, K., Hu, J.: "A Graph-Based Evolutionary Algorithm: Genetic Network Programming and Its Extension Using Reinforcement Learning", Evolutionary Computation, Vol. 15, No. 3, Fall 2007, pp. 369–398.

[9] Mabu, S., Hirasawa, K., Hu, J., Murata, J.: "Online Learning of Genetic Network Programming and Its Application to Prisoner's Dilemma Game", Transactions of IEE Japan, Vol. 123-C, No. 3, 2003, pp. 535-543.

[10] Katagiri, H., Hirasawa, K., Hu, J.: "Network Structure Oriented Evolutionary Model: Genetic Network Programming", Transaction of the Society of Instrument and Control Engineers, Vol. 38, No. 5, 2002, pp. 485-494.

MOBILITY & VEHICLE MECHANICS

DOI: 10.24874/mvm.2018.44.03.05
UDC: 629.016.2

OPTIMIZATION-BASED CONTROLLERS FOR HYBRID ELECTRIC VEHICLES

Giovanni Belingardi [1], Pier Giuseppe Anselma [2], Miroslav Demic [3]*

Received in August 2018 Accepted in October 2018

RESEARCH ARTICLE

ABSTRACT: Hybrid electric vehicles (HEVs) are more and more of interest in the present vehicle market, because of the relevant reduction both in the fuel consumption and in the CO_2 emission, in particular for the urban utilization. Different architectures are possible and have been considered for the vehicle hybridization. The most convenient architecture is depending on the application itself. This paper deals with a design methodology based on an optimization scheme to make the selection among the consistent number of alternatives. Optimization-based control strategies play a central role in the design process of HEVs. In early design phases they allow the comparison of different HEV powertrain architectures, thus supporting the selection of an appropriate topology. Furthermore, they lay the foundations for the development of real-time optimal energy management strategies to be implemented in the HEV on-board control unit. Fuel economy and design efficiency can overall be enhanced in this way. This paper aims at providing a comprehensive review of different optimization-based energy management strategies for HEVs. An analysis of strength and drawbacks of each considered strategy is carried out based on different evaluation criteria such as global optimality, computational cost and uniformity of the powertrain operation. Finally, simulation results for a HEV powertrain from the industrial state-of-art validate the conceptual and methodological comments related to the analysed controllers.

KEY WORDS: control optimization, fuel economy, hybrid electric vehicle, optimal design, powertrain modelling

[1]*Giovanni Belingardi, Prof., University in Turin, Politecnico di Torino – DIMEAS – Italy, 10129 Torino, giovanni.belingardi@polito.it (*Corresponding author)*
[2]*Pier Giuseppe Anselma, Ph.D., Student, University in Turin, Politecnico di Torino – DIMEAS – Italy, 10129 Torino, pier.anselma@polito.it*
[3]*Miroslav Demic, Prof., University of Kragujevac, Serbian Academy of Engineering Science, 34000 Kragujevac demic@kg.ac.rs*

KOTROLERI ZASNOVANI NA OPTIMIZACIJI ZA HIBRIDNA ELEKTRIČNA VOZILA

REZIME: Hibridna električna vozila (HEV) su sve više interesantna za sadašnje tržište vozila, zbog značajnog smanjenja u potrošnji goriva i emisije CO_2 gasova, posebno u urbanom okruženju. Koriste se različite arhitekture za hibridizaciju vozila. Najprikladnija arhitektura zavisi od same primene. Ovaj rad se bavi metodologijom projektovanja zasnovanoj na šemi optimizacije koja bira između konzistentnog broja alternativa. Strategije upravljanja zasnovane na optimizaciji imaju glavnu ulogu u procesu projektovanja HEV. U ranim fazama projektovanja oni omogućavaju poređenje različitih arhitektura HEV pogona, čime se podržava izbor odgovarajuće koncepcije. Osim toga, postavili su temelje za razvoj optimalnih strategija za upravljanje energijom u realnom vremenu koje se primenjuju u HEV upravljačkoj jedinici. Na taj način se može poboljšati ekonomičnost potrošnje goriva i efikasnost rešenja. Ovaj rad ima za cilj da obezbedi sveobuhvatan pregled različitih strategija upravljanja energijom HEV-a zasnovanih na optimizaciji. Analiza prednosti i nedostatka svake razmatrane strategije urađena je na osnovu različitih kriterijuma za ocenu, kao što su globalni optimum, troškovi proračuna i uniformnost rada pogonske grupe. Na kraju, rezultati simulacije HEV pogonske grupe sa stanovišta razvoja tehnologije industrijske proizvodnje potvrđuju konceptualne i metodološke rezultate vezane za analizirane kontrolere.

KLJUČNE REČI: optimizacije upravljanja, ekonomičnost potrošnje goriva, hibridno električno vozilo, optimalan dizajn, modeliranje pogonske grupe

OPTIMIZATION-BASED CONTROLLERS FOR HYBRID ELECTRIC VEHICLES

Giovanni Belingardi, Pier Giuseppe Anselma, Miroslav Demic

1. INTRODUCTION

Regulations to reduce motor vehicle CO2 emissions and fuel consumption have been enforced worldwide recently [1]. This stringent trend is expected to be confirmed and even made more severe over the next decades. Vehicle producers have been subsequently pushed to employ new technologies, including the use of fully electrified powertrains. In this framework, hybrid electric vehicles (HEVs) are establishing as one of the most promising solutions to satisfy customer requirements and CO2 emission regulations at the same time. A HEV adds an additional power source (e.g. battery, ultra-capacitor, etc.) and one or multiple actuators (i.e. electric machines) to the conventional powertrain. The additional power devices help to improve system efficiency and fuel economy by engine right-sizing, load levelling, regenerative braking and pure electric mode.

To design a HEV, the engineer typically first selects one configuration to focus on. The vehicle design parameters (e.g. motor size, battery size, planetary gear sizes, etc.) and control strategy then need to be determined. Obviously, to achieve the near-optimal overall performance for the selected configuration, an iterative process needs to be executed. However, the problem for this approach is that even with this optimal performance, it is not known whether the selected configuration offers the best solution among all possible configurations. To achieve this goal, the exact same process, beginning from the selection of another configuration and then iteratively approaching the optimal performance, has to be repeated. Moreover, only when the optimal performance is gained for each configuration, then the comparison between them is a sensible task. With numerous options for the configuration design variations, such an iterative process can only be developed by means of a systematic method with many underlying techniques, including the automated model generation and simulation with optimal design and optimal control techniques. The many different possible configurations and additional propulsion components bring new challenge and research opportunities to vehicle designers. As several control problems reported in the literature, the control of HEVs can have a two level hierarchical architecture: the lower level control, and the supervisory control. For the lower level control, each subsystem (e.g. engine, electric motors, battery) is equipped with actuators, sensors and a control system to regulate its behavior, in response to the supervisory control commands. The design of lower level controllers can be separated from the supervisory controller, and it will not be considered in this paper. The supervisory control of the HEVs determines the operating mode and power levels of all power devices to balance design objectives such as drivability, fuel economy and battery health. The supervisory level control and its use in assessing the optimality of design candidates are the focus of this paper. This paper is organized as follows: the different architectures for an HEV and its design process are presented. The optimization-based control strategies for HEVs are subsequently illustrated and analyzed. A case study for the assessment of these strategies is then presented. Conclusions are finally given.

2. THE HEV DESIGN PROCESS

2.1 HEV powertrain architectures

To date three main categories are identified for a HEV architecture: series, parallel and power-split. The correspondent block diagrams are illustrated in Figure 1.

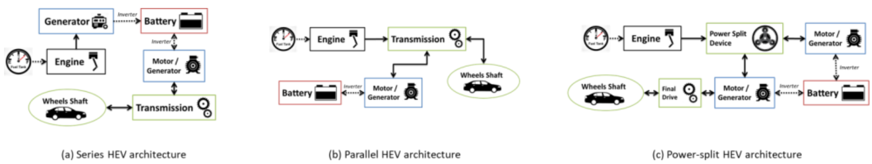

Figure 1. Different HEV architectures

2.1.1 Series HEV

In a series HEV, the propulsion is provided by one traction motor or more than one motors; the conventional engine drives the electricity generator, and they are both decoupled from the drivetrain. Since there is no mechanical coupling between the engine and vehicle drive axle, the engine speed and power are not rigidly constrained by the vehicle speed and road load, which enables the engine to operate always at high efficiency. In addition, because the traction motor usually can provide enough traction torque, transmission, in particular a gearbox, may not be needed. Despite simple and easy to control, the series hybrid vehicle powertrain suffers from high energy conversion losses: 100 % of the engine output must be converted into electrical power and some of it is further converted into electrochemical form and stored in the battery. The low efficiency is more pronounced when the vehicle is running in highway cruise or steady state because of double energy conversion (mechanical-electric-mechanical), while the series configuration is good for very transient drive cycles.

2.1.2 Parallel HEV

In a parallel HEV, both the electric Motor/Generator (MG) and the Internal Combustion Engine (ICE) can contribute to the propulsion directly. In other words, the engine torque and the electric motor torque are additive. When the MG is relatively small, it can only start/stop the engine, provide some regenerative power features, and drive the vehicle in limited circumstances; when the MG is large, it can drive the vehicle by itself or simultaneously with the engine. The MG can be used to shift the engine operating points to a higher-efficiency area by acting as a generator when the power demand is low or as a motor at high power demand. The efficiency of parallel hybrid vehicles can be very high on highways since the engine can directly drive the vehicle near its sweet spot and energy circulation between the mechanical energy and electric energy can be significantly reduced, while it reveals to be less convenient in transient driving cycles.

2.1.3 Power-split HEV

In a typical power-split HEV, an engine and two electric machines are connected to make a so-called “power-split device”, represented by one or multiple planetary gear (PG) sets, through the carrier, the sun gear, and the ring gear. The lever diagram can be used to represent the 2 degrees of freedom dynamics of a PG, as illustrated in Figure 2.

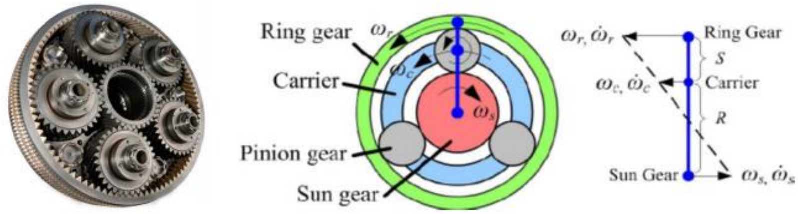

Figure 2. Planetary gear set and the lever diagram

The early power-split transmission appeared in the late 1960s and early 1970s, when such power-split mechanisms were used in lawn tractors. Although other early studies on power-split hybrid vehicles followed, at authors' best knowledge, in the market there was no passenger power-split hybrid vehicle until the Toyota Motor Corporation introduced the Prius, the first mass-production HEV in the world, in Japan in 1997 [2]. This hybrid powertrain system, called the Toyota Hybrid System (THS), is the framework and the foundation of all Toyota hybrid vehicles, as well as hybrid vehicles from several other companies, including the Ford Fusion Hybrid and the General Motor Allison Hybrid system [3]. Power-split hybrid vehicles are efficient in city driving conditions as a result of the pure electric drive function. However, due to energy circulation from the generator to the motor, the power-split vehicles may have higher energy losses than parallel HEVs in highway driving. This problem for single-mode power split hybrids can be avoided by adding clutch connections between different PG nodes, thus realizing multi-mode hybrid designs. Engagements and disengagements of clutch connections can enable different operating modes, thus improving the overall efficiency and performance of the system. Each operating mode typically best suits a specific case of vehicle operation (e.g. launching, accelerating, cruising at high speed, regenerative braking). Power-split architectures are the most successful and represent a large portion of the current population of HEVs. This paper particularly focuses on the power-split HEV powertrains with 2 PGs. A lever diagram for an example of this kind of system, taken from the industrial state-of-the-art, can be seen in Figure 3 [4]. The correspondent PG and final drive gear ratios are reported in the figure as well.

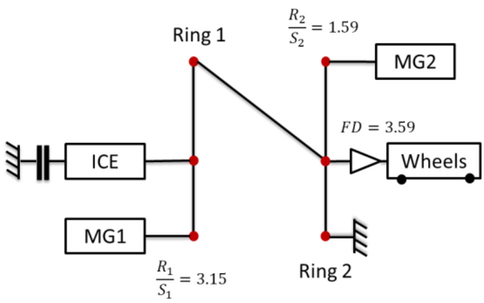

Figure 3. Example of a power split HEV

2.2 Modelling method for a power-split HEV

Many of today's power-split hybrid vehicles use two MGs to complement the ICE. In this paper, we only consider the case that each PG set is connected with two powertrain components, since having three powertrain components on the same PG will lead to very limited design flexibility. If we consider only the cases in which the engine and output shaft are on different PGs and each is complemented by a MG (inspired by Prius and GM Volt Gen 2), there are 144 possible configurations for components location. Three examples of configurations are reported in Figure 4.

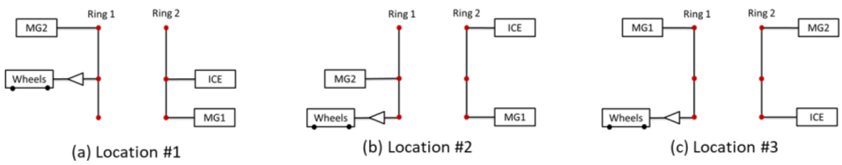

Figure 4. Examples of different components location for a 2 PG HEV

N_{clutch}, the total number of possible clutches, results to be 16. This value is found by using equation (1) and considering the number of PG sets (N_p) equal to 2. A correspondent graphical interpretation can be seen in Figure 5.

$$N_{clutch} = (C_{2N_p} - 2N_p) + 3N_p - 1 \tag{1}$$

The first parenthesized term (C_{2N_p}) represents the possible clutches added between each pair of nodes and corresponds to 15 for a double PG set. The second parenthesized term represents the redundant clutches to be eliminated. Since only one clutch could lock a planetary gear set by connecting any two nodes out of three in that planetary gear set, the other two possible connections are redundant (displayed in red in Figure 5). $3N_p$ represents the grounding clutches: all the gear nodes could be grounded except the one attached to output, eliminated by the last term.

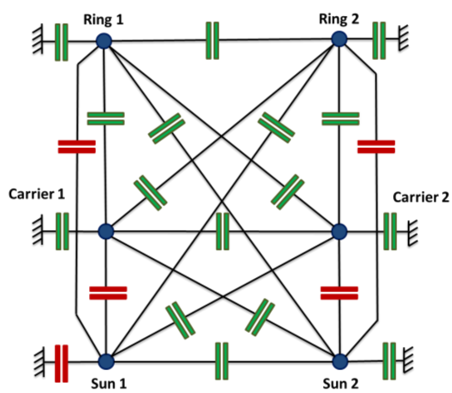

Figure 5. All possible clutch locations of a double PG HEV

Setting the maximum number of clutches to 3, this leads to generate 7280 different designs for each location of components. Therefore, the total number of candidate transmission designs (144x7280) for each set of input parameters is more than one million [5].

A methodology to model the modes of multi-mode HEVs was proposed in [6]. The dynamics of any specific mode is described by the characteristic matrix [A*], as shown in equation (2). This 4x4 characteristic matrix [A*] governs the relationship between the angular acceleration of powertrain components and their corresponding torques. The detailed derivations have been described by X. Zhang *et al.* in [6].

$$\begin{bmatrix} \dot{\omega}_{ICE} \\ \dot{\omega}_{OUT} \\ \dot{\omega}_{MG1} \\ \dot{\omega}_{MG2} \end{bmatrix} = [A^*] \begin{bmatrix} T_{ICE} \\ T_{OUT} \\ T_{MG1} \\ T_{MG2} \end{bmatrix} = \begin{bmatrix} a_{11} & a_{12} & a_{13} & a_{14} \\ a_{21} & a_{22} & a_{23} & a_{24} \\ a_{31} & a_{32} & a_{33} & a_{34} \\ a_{41} & a_{42} & a_{43} & a_{44} \end{bmatrix} \begin{bmatrix} T_{ICE} \\ T_{OUT} \\ T_{MG1} \\ T_{MG2} \end{bmatrix} \tag{2}$$

2.3 Engine model

The ICE can be taken into account through its experimental furl flow map. This fuel map is the result of the adopted electronic fuel injection system's setting for regulating the air/fuel mix and is created by engineers during the construction and tests of an engine. This lookup table represents a summary of the engine’s entire operating regime with respect to torque and speed. For supervisory control studies and fast prototype design, the engine transient dynamics due to spark-timing and fuel injection are ignored.

2.4 Electric motors model

The two motor/generators assisting the thermal engine in the powertrain model are direct current machines. In our transmission model, the size and performances of the electric machines is not a design parameter, but rather an optimization parameter. This means that a model of the losses in the electric machines is not required, but rather the electric machines are already existing and manufactured. Their implementation in the transmission model goes through their correspondent loss map, which can be empirically obtained from measurement tests on the real machines. For every possible combination of torque and speed, the loss map returns the measured lost power of the electric machine.

2.5 Battery model

Based on the dynamic characteristics and working principles of the battery, the equivalent circuit model was developed by using resistors, capacitors and voltage sources to form a circuit network. In this paper we use the Rint model, which is the most popular battery model for studying hybrid powertrain design due to its capacity to simulate battery dynamics while having a simple approach. The Rint model implements an ideal voltage source V_{OC} to define the battery open-circuit voltage, together with an internal resistance R_{IN}. The variation in time of the battery State-of-Charge (SOC), $S\dot{O}C$, can thus be expressed as

$$S\dot{O}C = \frac{\sqrt{{V_{OC}}^2 - 4 \cdot R_{IN} \cdot P_{batt}} - V_{OC}}{2 \cdot R_{IN} \cdot Q_{batt}} \tag{3}$$

where P_{batt} and Q_{batt} represent the power requested from the battery and its capacity, respectively. P_{batt} can be evaluated from the power requested or provided by the MGs, adding the correspondent values of lost power from the experimental maps.

3. OPTIMIZATION-BASED HEV CONTROL

In order to assess the millions of HEV powertrain configurations above generated, a proper control strategy needs implementation. In early vehicle design phases, the powertrain operation is optimized offline. In other words, the trajectory of the vehicle speed is known a priori and it is determined by standard duty cycles (e.g. the New European Driving Cycle (NEDC), the Urban Dynamometer Driving Schedule (UDDS)). This contrasts with actual real driving conditions, where the powertrain control unit does not have input information concerning the future operating conditions. In offline HEV control, optimization-based control approaches can be adopted to estimate the fuel consumption of each analysed powertrain design and consequently identify the optimal one.

In general, three main approaches can be identified related to offline optimization of multimode power split HEVs:

1. The Pontryagin's Minimum Principle (PMP)
2. Dynamic Programming (DP)
3. The Power-weighted Efficiency Analysis for Rapid Sizing (PEARS)

All these approaches aim at analysing the HEV performance in Charge-Sustaining (CS) mode, having the battery SOC with equal values at the beginning and at the ending of the optimization time horizon.

3.1 The Pontryagin's Minimum Principle

The PMP is a general case of the Euler-Lagrange equation in the calculus of variation. It optimizes a single operating trajectory for the HEV powertrain, thus achieving local optimal solutions without guaranteeing global optimality [7]. The algorithm is dived into two steps: an inner-loop problem solved at each time point of the considered drive cycle, and a time-horizon control problem.

3.1.1 Inner-loop problem

Before solving the control problem for the overall considered drive cycle, an inner-loop optimization process is performed to obtain the family of the best ICE operating points correspondent to specific values of output torque and speed. Firstly, P_{batt} and the fuel consumption $\dot{m}_{fuel}$ are evaluated as a function of the ICE torque and speed values (T_{ICE} and ω_{ICE}, respectively) in (4).

$$P_{batt} = h(\omega_{ICE}, T_{ICE}) \tag{4}$$

The inner-loop optimal problem to minimize the fuel consumption subject to a defined battery power is then defined as

$$\min \left[\dot{m}_{fuel} = L\,(\omega_{ICE}, T_{ICE}) \right] \tag{5}$$

$$\text{Subject to } \; h(\omega_{ICE}, T_{ICE}) - P_{batt} = 0$$

The optimized control variables (i.e. T_{ICE} and ω_{ICE}) can thus be defined by choosing a point of minimal fuel consumption on each feasible ICE operating line as per P_{batt}. Figure 6 illustrates all the possible operating points for the inner-loop optimization problem, discriminating between pure electric and hybrid points whether the ICE is used or not. The optimal operating points are represented in Figure 6 by the lower edge of the blue points cloud.

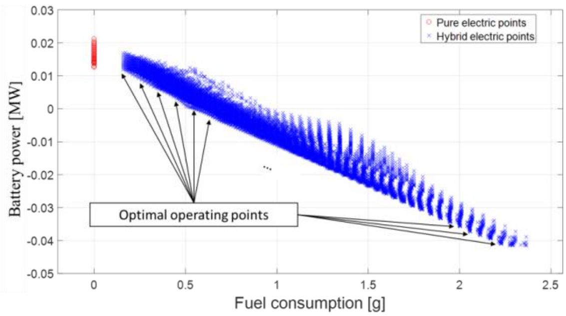

Figure 6. Instantaneous fuel consumption points for specific required output torque and speed values

In the time-horizon optimal control, this process reduces the bi-dimensional control variable (T_{ICE} and ω_{ICE}) to the single dimension ofP_{batt} only. The fuel consumption rate $\dot{m}_{fuel}$ can thus be determined fromP_{batt}, which could be decided by an on-board supervisory algorithm. The optimal ICE operating points in Figure 6 can be interpreted as a sort of Pareto frontier with a clear physical interpretation: in the best operating conditions, less battery power is needed when more fuel is consumed and viceversa.

3.1.2 Time-horizon control problem

From the assistance of the inner-loop optimal solutions, only is the control variable that decides all the operating points in the time-horizon plane of the optimal control problem. This variable sets the fuel consumption rate and the ICE operating point, which subsequently fixes all the other system variables such as the speed and torque of the MGs and the transmission status. The time-horizon control problem can thus be defined as

$$\min \; J = \int_{t\_0}^{t\_end} g(P_{batt}, t)\, dt$$

$$\text{Subject to} \quad \dot{SOC} = \mathrm{f}(\mathrm{SOC}, P_{batt}) \qquad (6)$$

$$SOC(t_0) = SOC(t_{end})$$

where g is the best fuel consumption rate according to Figure 6. The optimal control variable in the PMP is obtained minimizing a performance measure, which is defined as a Hamiltonian H. Its mathematical formulation is illustrated in (7)

$$\mathrm{H} = \mathrm{g}(P_{batt}, t) + \lambda \cdot \dot{SOC} \qquad (7)$$

where λ is a constant co-state variable that can be tuned to achieve the optimal control objective. Recent studies illustrated different methods to properly tune this parameter, obtaining fuel economy results consistently comparable with the global optimum [7, 8]. However, accuracy may be questionable when the operating conditions change. Moreover, tuning the equivalence factor may result computationally inefficient when dealing with component sizing in the HEV powertrain design procedure.

3.2 Dynamic Programming

The DP approach is by far the currently most applied approach for HEV control. The concept of DP was proposed by Richard Bellman in the 1940s and refined by Bellman himself in 1954 [9]. This global optimization method was firstly introduced to the HEV problem by H. Mosbech in the 1980s [10]. However, because it was constrained by the computation power available at that time, this approach did not draw much attention until the later work by Brahma et al. in 2000 [11]. Since then, this topic has been studied extensively and was extended to power-split HEVs by Liu in 2006 [12]. The DP approach guarantees global optimality through an exhaustive search of all control and state grids. Its process is implemented backward from the final drive cycle time point to the initial one by searching for the optimal trajectory among the discretized grid points, as illustrated in Figure 7. Particularly, the Bellman's principle of optimality states that the optimal policy can be obtained if a single-stage sub-problem involving only the last stage is solved first, then the sub-problem involving the last two stages, last three stages, etc. until the entire problem is solved step by step.

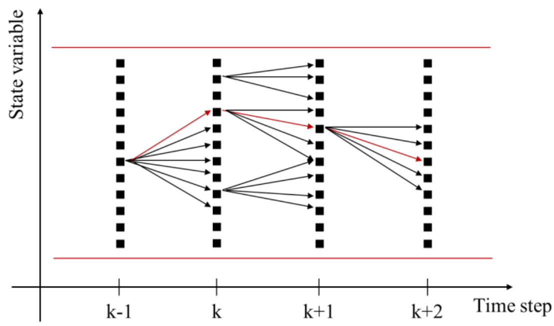

Figure 7. Dynamic programming process

For the HEV control problem, this signifies the minimization of the cost function J defined in equation (8) over the considered time horizon.

$$J = \sum_{k=0}^{N-1} \left(\dot{m}_{fuel_k} + \alpha \cdot \Delta SOC^2\right)$$

$$\Delta SOC = \begin{cases} SOC_k - SOC_{target} & SOC_k < SOC_{target} \\ 0 & SOC_k \geq SOC_{target} \end{cases} \qquad (8)$$

SOC_{target} is the desired value of battery SOC, while α represents an operating factor. DP is demonstrated to achieve global optimality under a wide range of operating conditions, but its major drawback refers to the computational power needed for exhaustively searching through all the possible solutions and tuning α.

3.3 Power-weighted Efficiency Analysis for Rapid Sizing

The Power-weighted Efficiency Analysis for Rapid Sizing (PEARS) has been introduced by Zhang et al. as a rapid near-optimal control strategy for HEVs [13]. In the PEARS algorithm, mode overall efficiency values are retained as the weighting factor for selecting hybrid or electric powertrain operation. Beforehand, speed and torque of power components are swept to determine the optimal combination in terms of mode efficiency at each driving cycle point. The overall mode efficiency values to maximize (η_{EV} and η_{HEV}) are illustrated in (9) for pure electric and hybrid modes, respectively.

$$\eta_{EV} = 1 - \frac{P_{EV}^{loss}}{P_{EV}^{in}}$$

$$\eta_{HEV} = \frac{P_{ICE\_1}\eta_G\eta_{batt}/(\eta_{ICE\_max}\eta_{G\_max})}{P_{fuel} + \mu P_{batt}} + \frac{P_{ICE\_2}\eta_G\eta_M/(\eta_{ICE\_max}\eta_{G\_max}\eta_{M\_max})}{P_{fuel} + \mu P_{batt}} + \frac{\frac{P_{ICE\_3}}{\eta_{ICE\_max}} + \mu P_{batt}\eta_{batt}\eta_M/\eta_{M\_max}}{P_{fuel} + \mu P_{batt}} \quad (9)$$

For the electric modes, P_{EV}^{loss} includes both battery loss and electric drive loss, and P_{EV}^{in} refers to the power flowing into the system. For the hybrid modes, all the possible power flows are illustrated in Figure 8. P_{ICE_1} is the engine power from the engine through the generator to the battery, P_{ICE_2} is the engine power that flow from the engine through the generator to the motor, $P_{ICE_3}$is the engine power that flows directly to the final drive. $P_{ICE\_1} + P_{ICE\_3} + P_{ICE\_3}$ is the total engine power, P_{batt} is the battery power and μ is a flag for battery assist. P_{fuel} is the rate of fuel energy injected; subscripts G and M refer to generator (when the power is negative) and motor (when the power is positive or zero). η_{ICE_max}, η_{G_max}, and η_{M_max} are the highest efficiency of the engine, the generator, and the motor, respectively.

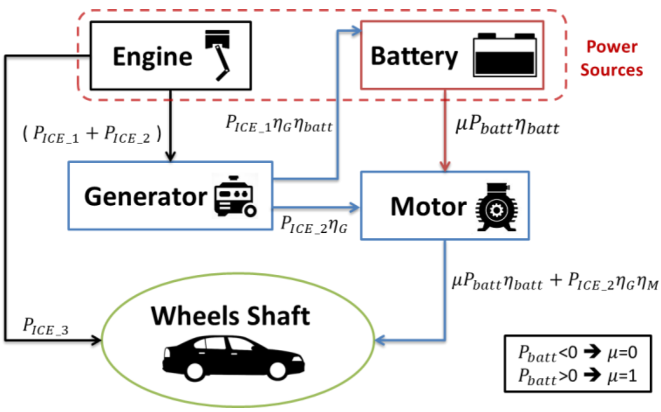

Figure 8. Power flow in the hybrid modes

Once the entire driving cycle is analyzed to extract the optimal power split for each operating mode at each time step, the powertrain is initially set to operate in electric modes only (the most efficient one according to speed and torque output). Subsequently, a recursive process starts that aims at replacing electric with hybrid operation in the driving cycle points where the smallest ranges between hybrid and electric mode efficiencies are observed. This iterative procedure is conducted until charge-balance is realized and the battery State-of-Charge (SoC) exhibits equal values at the beginning and at the end of the driving cycle. The mode-shifting schedule and the resulting fuel consumption can be evaluated in this way. Details regarding the operation of the algorithm can be found in [14].

The PEARS algorithm was demonstrated to be able to obtain results similar to Dynamic Programming (DP), while being over 10000 times faster [15] The issue with implementing a PEARS technique is that it generates an unrealistic mode-shifting schedule. To overcome this drawback, the authors of the algorithm tried to combine PEARS with DP: more uniform mode-shifting schedules were obtained, however computational cost was increased at the same time [14]. Anselma et al. [14] detected and analyzed the problematic points of the PEARS algorithm. Subsequently, a solution to minimize mode-shifting events was proposed without excessive increase of the computational cost.

4. CASE STUDY

After having presented the majorly employed optimization-based controllers for HEVs, this session presents a case study to assess the advantages and drawbacks of each control strategy. The analysed vehicle data are reported in Table 1, while the powertrain layout corresponds to the one of Figure 3.

Table 1. Vehicle parameters

Component	Parameters
Engine	188 kW @ 5800 rpm 320 Nm @ 4400 rpm
$P_{MG1_{max}}$ [kW]	60
$P_{MG2_{max}}$ [kW]	85
Final Drive Ratio	3.59
$R_1 : S_1$	3.15
$R_2 : S_2$	1.59
Vehicle Mass [kg]	2248

All the three control strategies presented above were implemented and simulated in MATLAB© software. In general, a quasi-static approach was adopted considering the time step equal to 1 second. The UDDS driving cycle profile was retained as a good representative of the urban driving conditions. The correspondently obtained results for the fuel consumption trends and battery SOC trajectories can be seen in Figure 9. Table 2 reports the calculated total fuel consumption values and the correspondent computational time considering a desktop computer with Intel Core i7-8700 (3.2 GHz) and 32 GB of RAM.

Table 2. Simulation results

Control strategy	UDDS fuel consumption [g]	Computational time [minutes]
DP	258	5
PMP	261	4
PEARS	284	2

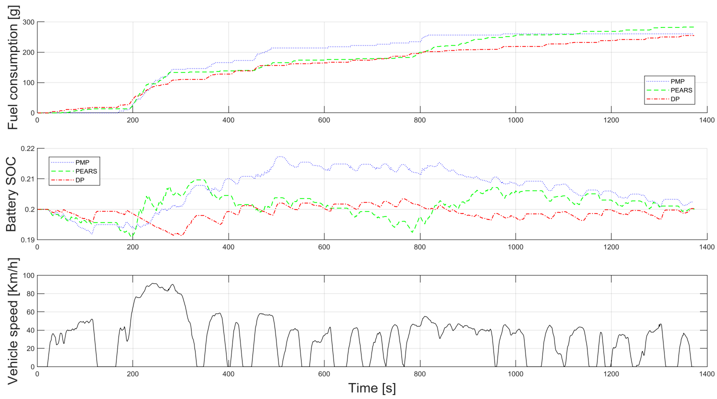

Figure 9. Simulation results for the control strategies in UDDS

Simulation results confirm the capability of reaching global optimal fuel economy employing a DP approach. On the other hand, PMP and PEARS establish themselves as near-optimal control strategies for HEVs, with the correspondent fuel economy predicted values increased by 1.16 % and 11.1% respectively. In this particular case study, the performance achieved by the PEARS algorithm in fuel economy is lightly lower than its major competitors. This is due to the PEARS especially designed for HEV powertrains with several operating modes, where it is able to realize consistent fuel economy with DP [15].On the other hand, the HEV powertrain considered in [17]*Error! Reference source not found.* can operate only one electric mode and one hybrid mode, thus compromising the flexibility and freedom to operate of PEARS. However, the PEARS achieves interesting results in terms of computational efficiency being the most rapid control strategy to determine the powertrain operating schedule. Indeed, DP requires consistently increased computational effort to evaluate the global optimal solution for the HEV control problem, while PMP represents a trade-off between the other two approaches in this sense.

5. CONCLUSIONS

In this paper, references are provided concerning the different powertrain architectures for HEVs. A modelling and optimization technique for power split HEV powertrains is illustrated, which include analytical formulations for the transmission and experimental tables for the power components.

The three mainly adopted optimization-based control techniques for HEVs (i.e. PMP, DP and PEARS) are subsequently presented and their mathematical formulations are analysed. These strategies are then simulated considering the operation of a HEV powertrain design from the industrial state-of-art in the urban driving cycle. Results show that the DP is effectively capable of achieving global optimal performance in terms of fuel economy. On their behalf, PMP and PEARS demonstrate near-optimal fuel economy results while increasing the computational efficiency. The control strategy to adopt in the HEV design process depends on the peculiar application. The PEARS algorithm reveals particularly efficient for optimizing power split HEVs with multiple operating modes, due to its ease of implementation and flexibility in the operation. Moreover, its computational rapidness represents a consistent advantage when analysing millions of different HEV powertrain configurations. On the other hand, employment of DP and PMP may be suggested for the cases of HEV powertrains with a limited number of different operating modes, since they can efficiently predict optimal fuel economy values. The optimization of a HEV architecture may demonstrate significantly improved when the accuracy of the vehicle model is increased. As an example, micro and macro road profiles may replace the standard driving cycles to simulate real-world driving conditions [15]. Moreover, including the position and the characteristics of the powertrain may be accounted as well to reduce the negative effects of vibrations [16]. Finally, the optimization reliability can be consistently enhanced when the physical perception and the behaviour of the driver are included in the model [17, 18].

REFERENCES

[1] Regulation (EU) No 333/2014 of the European Parliament and of the Council of 11 March 2014 amending Regulation (EC) No 443/2009 to define the modalities for reaching the 2020 target to reduce CO2 emissions from new passenger cars, April 2014.

[2] Liu, J., Peng, H., Filipi, Z.S.: “Modeling and Analysis of the Toyota Hybrid System”, Proceedings of the 2005 IEEE/ASME International Conference on Advanced Intelligent Mechatronics, 24-28 July, Monterey, USA, 2005.

[3] Arata, J., Leamy, M., Meisel, J., Cunefare, K., Taylor, D.: "Backward-Looking Simulation of the Toyota Prius and General Motors Two-Mode Power-Split HEV Powertrains", SAE Int. J. Engines, Vol. 4, No. 1, pp 1281-1297, 2011.

[4] Pittel, M., Martin, D.: “eFlite Dedicated Hybrid Transmission for Chrysler Pacifica”, SAE Technical Paper 2018-01-0396, 2018.

[5] Anselma, P.G., Huo, Y., Roeleveld, J., Emadi, A., Belingardi, G.: “Rapid optimal design of a multimode power split hybrid electric vehicle transmission”, Proceedings of the Institution of Mechanical Engineers, Part D: Journal of Automobile Engineering, online Jan. 2018.

[6] Zhang, X., Li, S., Peng, H., Sun, J.: “Efficient Exhaustive Search of Power Split Hybrid Powertrains with Multiple Planetary Gears and Clutches”, Journal of Dynamic Systems Measurement and Control, Vol. 137, No. 12, 2015.

[7] Kim N., Cha, S., Peng, H., "Optimal Control of Hybrid Electric Vehicles Based on Pontryagin's Minimum Principle", in IEEE Transactions on Control Systems Technology, Vol. 19, No. 5, Sept. 2011, pp. 1279-1287.

[8] Kim, N., Rousseau, A.: “Sufficient conditions of optimal control based on Pontryagin’s minimum principle for use in hybrid electric vehicles”, Proceedings of the Institution of Mechanical Engineers, Part D: Journal of Automobile Engineering, Vol 226, Issue 9, 2012, pp 1160 – 1170.

[9] Bellman, R.: “The Theory of Dynamic Programming”, Bulletin of American Mathematical Society, 1954.

[10] Mosbech, H.: "Optimal control of hybrid vehicle", Proceedings of the Int. Symp. Automotive Technology Automation (ISATA '80), Vol 2, 1980, pp 303-320.

[11] Brahma A., Guezennec, Y., Rizzoni, G.: "Optimal Energy Management in Series Hybrid Electric Vehicles," in American Control Conference, Chicago, IL, 2000.

[12] Liu, J. Peng, H.: "Control optimization for a power-split hybrid vehicle," in American Control Conference, Minneapolis, MN, 2006.

[13] Zhang, X., Peng, H., Sun, J.: “A near-optimal power management strategy for rapid component sizing of power split hybrid vehicles with multiple operating modes”, in American Control Conference (ACC), 2013, Washington, DC, USA, pp 5972-5977.

[14] Anselma, P.G., Huo, Y., Amin, E., Roeleveld, J., Emadi, A., Belingardi, G.: “Mode-shifting Minimization in a Power Management Strategy for Rapid Component Sizing of Multimode Power Split Hybrid Vehicles,” SAE Technical Paper 2018-01-1018, 2018.

[15] Demic, M., Diligenski, D., Demic, I.: “New design of a road profiler”, International Journal of Automotive Technology, Vol. 11, No. 6, 2010, pp 801-808.

[16] Demić, M.: “Contribution to the optimization of the position and the characteristics of passenger car powertrain mounts”, International Journal of Vehicle Design, Vol. 11, No. 1, 1990, pp 87-103.

[17] Demić, M.: “Optimization of Vehicles Elasto-Damping Elements Characteristics from the Aspect of Ride Comfort, Vehicle System Dynamics”, International Journal of Vehicle Mechanics and Mobility, Vol. 23, No. 1, 1994, pp 351-377.

[18] Demic, M., Lukic, J.: “Investigation of the transmission of fore and aft vibration through the human body”, Applied Ergonomics, Vol. 40, No. 4, 2009, pp 622-629.

Intentionally blank

MVM – International Journal for Vehicle Mechanics, Engines and Transportation Systems

NOTIFICATION TO AUTHORS

The Journal MVM publishes original papers which have not been previously published in other journals. This is responsibility of the author. The authors agree that the copyright for their article is transferred to the publisher when the article is accepted for publication.

The language of the Journal is English.

Journal ***Mobility & Vehicles Mechanics*** is at the SSCI list.

All submitted manuscripts will be reviewed. Entire correspondence will be performed with the first-named author.

Authors will be notified of acceptance of their manuscripts, if their manuscripts are adopted.

INSTRUCTIONS TO AUTHORS AS REGARDS THE TECHNICAL ARRANGEMENTS OF MANUSCRIPTS:

Abstract is a separate Word document, "*First author family name_ABSTRACT.doc*". Native authors should write the abstract in both languages (Serbian and English). The abstracts of foreign authors will be translated in Serbian.

This document should include the following: 1) author's name, affiliation and title, the first named author's address and e-mail – for correspondence, 2) working title of the paper, 3) abstract containing no more then 100 words, 4) abstract containing no more than 5 key words.

The manuscript is the separate file, „*First author family name_Paper.doc*" which includes appendices and figures involved within the text. At the end of the paper, a reference list and eventual acknowledgements should be given. References to published literature should be quoted in the text brackets and grouped together at the end of the paper in numerical order.

Paper size: Max 16 pages of B5 format, excluding abstract
Text processor: Microsoft Word
Margins: left/right: mirror margin, inside: 2.5 cm, outside: 2 cm, top: 2.5 cm, bottom: 2 cm
Font: Times New Roman, 10 pt
Paper title: Uppercase, bold, 11 pt
Chapter title: Uppercase, bold, 10 pt
Subchapter title: Lowercase, bold, 10 pt
Table and chart width: max 125 mm
Figure and table title: Figure _ (Table _): Times New Roman, italic 10 pt

Manuscript submission: application should be sent to the following e-mail:

mvm@kg.ac.rs ; lukicj@kg.ac.rs
or posted to address of the Journal:
University of Kragujevac – Faculty of Engineering
International Journal M V M
Sestre Janjić 6, 34000 Kragujevac, Serbia

The Journal editorial board will send to the first-named author a copy of the Journal offprint.

OBAVEŠTENJE AUTORIMA

Časopis MVM objavljuje orginalne radove koji nisu prethodno objavljivani u drugim časopisima, što je odgovornost autora. Za rad koji je prihvaćen za štampu, prava umnožavanja pripadaju izdavaču.

Časopis se izdaje na engleskom jeziku.

Časopis ***Mobility & Vehicles Mechanics*** se nalazi na SSCI listi.

Svi prispeli radovi se recenziraju. Sva komunikacija se obavlja sa prvim autorom.

UPUTSTVO AUTORIMA ZA TEHNIČKU PRIPREMU RADOVA

Rezime je poseban Word dokument, "*First author family name_ABSTRACT.doc*". Za domaće autore je dvojezičan (srpski i engleski). Inostranim autorima rezime se prevodi na srpski jezik. Ovaj dokument treba da sadrži: 1) ime autora, zanimanje i zvanje, adresu prvog autora preko koje se obavlja sva potrebna korespondencija; 2) naslov rada; 3) kratak sažetak, do 100 reči, 4) do 5 ključnih reči.

Rad je poseban fajl, „*First author family name_Paper.doc*" koji sadrži priloge i slike uključene u tekst. Na kraju rada nalazi se spisak literature i eventualno zahvalnost. Numeraciju korišćenih referenci treba navesti u srednjim zagradama i grupisati ih na kraju rada po rastućem redosledu.

Dužina rada: Najviše 16 stranica B5 formata, ne uključujući rezime
Tekst procesor: Microsoft Word
Margine: levo/desno: mirror margine; unurašnja: 2.5 cm; spoljna: 2 cm, gore: 2.5 cm, dole: 2 cm
Font: Times New Roman, 10 pt
Naslov rada: Velika slova, bold, 11 pt
Naslov poglavlja: Velika slova, bold, 10 pt
Naslov potpoglavlja: Mala slova, bold, 10 pt
Širina tabela,dijagrama: max 125 mm
Nazivi slika, tabela: Figure __ (Table _): Times New Roman, italic 10 pt

Dostavljanje rada elektronski na E-mail: **mvm@kg.ac.rs ; lukicj@kg.ac.rs**

ili poštom na adresu Časopisa
Redakcija časopisa M V M
Fakultet inženjerskih nauka
Sestre Janjić 6, 34000 Kragujevac, Srbija

Po objavljivanju rada, Redakcija časopisa šalje prvom autoru jedan primerak časopisa.

MVM *Editorial Board*
University of Kragujevac
Faculty of Engineering
Sestre Janjić 6, 34000 Kragujevac, Serbia
Tel.: +381/34/335990; Fax: + 381/34/333192
www.mvm.fink.rs